Palaeogeography, Palaeoclimatology, Palaeoecology xxx (xxxx) xxxx

Contents lists available at ScienceDirect

Palaeogeography, Palaeoclimatology, Palaeoecology

journal homepage: www.elsevier.com/locate/palaeo

Diatom paleolimnology of late Pliocene Baringo Basin (Kenya) paleolakes

Karlyn S. Westover[a,*], Jeffery R. Stone[a], Chad L. Yost[b], Jennifer J. Scott[c], Andrew S. Cohen[b], Nathan M. Rabideaux[d,e], Mona Stockhecke[f,g], John D. Kingston[h]

[a] Department of Earth and Environmental Systems, Indiana State University, Terre Haute, IN, 47809, USA
[b] Department of Geosciences, University of Arizona, Tucson, AZ, 85721, USA
[c] Department of Earth and Environmental Sciences, Mount Royal University, Calgary, AB, T3E 6K6, Canada
[d] Department of Geosciences, Georgia State University, Atlanta, GA, 30302, USA
[e] Department of Chemistry, Rutgers University-Newark, Newark, NJ, 07109, USA
[f] University of Minnesota-Duluth, Duluth, MN, 55812, USA
[g] EAWAG Swiss Federal Institute of Aquatic Science and Technology, Duebendorf, Switzerland
[h] Department of Anthropology, University of Michigan, Ann Arbor, MI, 48109, USA

ARTICLE INFO

Keywords:
Paleoclimate
Diatomite
Biogenic silica
Alkaline lakes
East African rift

ABSTRACT

Kenya's Baringo-Tugen Hills-Barsemoi drill site is one of six localities across Kenya and Ethiopia from which the Hominin Sites and Paleolakes Drilling Project has obtained sediment cores in an effort to investigate the role of environmental forcing in shaping human evolution. The Baringo Basin site features extensive exposures of the Chemeron Formation, which contains > 100 fossil vertebrate localities including five hominin sites. The 228-m drill core, dating from ~3.29 to 2.56 Ma, is characterized by fluvio-lacustrine sediments, including multiple diatomites, with evidence of variable degrees of later pedogenic modification. In the lower part of the core (~3.29–3.04 Ma), diatoms were preserved only in very low abundance, consistent with predominantly fluvial or lake marginal environments. In contrast, five diatomites and two additional diatom-rich intervals were deposited after ~3.04 Ma, reflecting a major shift in the basin hydrology. Planktonic freshwater species dominated these diatom-rich intervals, whereas periphytic taxa were present in proportions less than 2%, suggesting that these intervals represent open-water deposition during lake highstands. Littoral or saline assemblages are largely absent throughout the core. Instead, we observed a pattern of increasing diatom frustule dissolution at the tops and bottoms of diatomite units, indicating increased alkalinity during the transgressive/regressive phases. A Na-bearing zeolite (analcime) indicative of saline waters precipitated in clastic-dominated intervals between diatomites, suggesting extreme environmental variability between lake highstands and lowstands. Diatom assemblages were consistently dominated by a few species belonging to the genera *Aulacoseira* and *Stephanodiscus*, which were at times co-dominant. We infer that assemblages dominated by *Aulacoseira* represent a well-mixed lake with abundant supply of silica. When *Stephanodiscus* was dominant, which occurred more frequently in the later freshwater phases, we infer incomplete mixing and reduced silica flux to the epilimnion (upper water layer).

1. Introduction

Lakes are valuable repositories of environmental history. The physical characteristics and geochemical and biological components of lake sediments reflect many processes operating at various spatial and temporal scales (Cohen, 2003). Diatoms (Bacillariophyceae) are a large and diverse group of single-celled microscopic algae found in freshwater and marine systems. They are especially useful as biological indicators of environmental change because they produce silica cell walls that are often preserved in sediments. Species are sensitive to chemical parameters such as pH, alkalinity, conductivity/salinity, and nutrient concentrations, as well as physical parameters such as convective mixing and light (Battarbee et al., 2001; Smol and Stoermer, 2010).

Paleolimnological studies are often used to infer past climate change because of the influence of climate on lake conditions and processes.

* Corresponding author.
E-mail addresses: karlyn.westover@indstate.edu (K.S. Westover), jeffery.stone@indstate.edu (J.R. Stone), chadyost@email.arizona.edu (C.L. Yost), jescott@mtroyal.ca (J.J. Scott), cohen@email.arizona.edu (A.S. Cohen), nathan.rabideaux@rutgers.edu (N.M. Rabideaux), mstockhe@d.umn.edu (M. Stockhecke), jkingst@umich.edu (J.D. Kingston).

https://doi.org/10.1016/j.palaeo.2019.109382
Received 20 March 2019; Received in revised form 9 September 2019; Accepted 11 September 2019

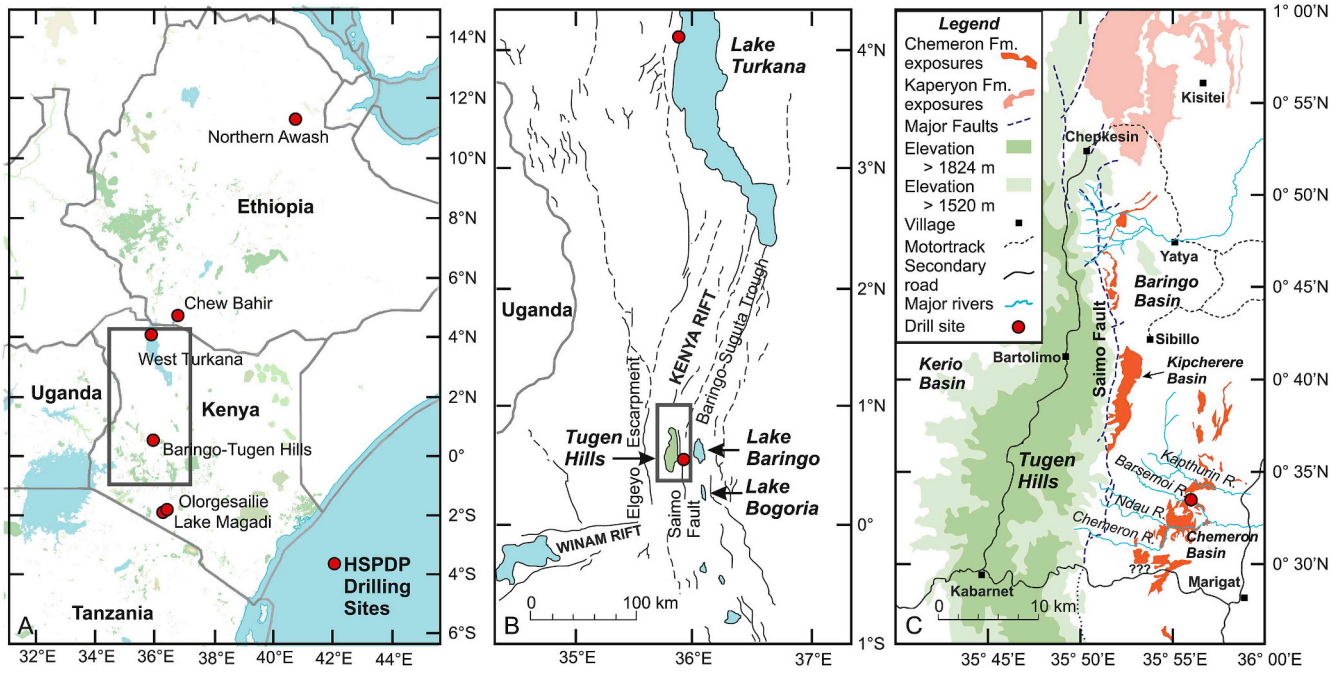

Fig. 1. A) Distribution of HSPDP drill sites in Ethiopia and Kenya (box = Fig. 1B); B) Tugen Hills, Lake Baringo, and Lake Bogoria in the Central Kenya Rift (box = Fig. 1C); C) Baringo Basin-Tugen Hills field area and the BTB13-1A core drilling site (red circle). Deino et al. (2006) and Kingston et al. (2007) described diatomites exposed in outcrops of the Chemeron Formation located < 1 km from the drilling site along the Barsemoi River. Fig. 1B & C adapted from Kingston et al. (2007). (For interpretation of the references to colour in this figure legend, the reader is referred to the Web version of this article.)

This has included studies of extant old, deep lakes found in tectonic basins, including Lake Malawi (Stone et al., 2011) and Lake Tanganyika (Burnett et al., 2011; Scholz et al., 2003) in East Africa. The same principles have also been extended to the study of paleolake sediments from lakes that no longer exist (e.g., Gasse, 1980; Kingston et al., 2007; Vilaclara et al., 1997) or exposed sediments deposited during Pleistocene highstands of extant lakes (e.g., Bergner and Trauth, 2004).

The Hominin Sites and Paleolakes Drilling Project (HSPDP) has produced multiple diagnostic paleorecords from drill cores, including those of fossil diatoms, to provide detailed, local paleoenvironmental inferences for important hominin fossil sites associated with the drilled sequences (Campisano et al., 2017; Cohen et al., 2016). Paleoecological evidence provided by diatoms contributes to evaluations of hypotheses of environmental factors that may have influenced human evolution. The Baringo-Tugen Hills-Barsemoi (BTB) site in Kenya (Fig. 1) is one of six paleolake sites investigated by the HSPDP.

The focus of the present study is the paleolimnological record of the diatom-bearing lacustrine deposits of a portion of the Chemeron Formation dating to the late Pliocene. This research follows an earlier investigation that mapped and sampled multiple Chemeron Formation diatomites exposed in outcrops along the eastern foothills of the Tugen Hills, in E-W trending drainages of the Barsemoi, Ndau, and Chemeron rivers (Fig. 1C). The 3 to 7 m thick 'Barsemoi' diatomites are composed of exclusively deep, freshwater assemblages and represent repeated lake cycles within the Baringo Basin between 2.7 and 2.55 Ma (Deino et al., 2006; Kingston et al., 2007). As part of HSPDP, the Baringo-Tugen Hills-Barsemoi core (BTB13-1A; 0.55458°N, 35.93748°E) was drilled adjacent to outcrop exposures of upper Chemeron sediments with the objective of more completely documenting the paleoenvironmental history of the basin during this interval (Cohen et al., 2016).

2. Geologic setting

The East African Rift System (EARS) is presently composed of a series of narrow faulted half-grabens oriented roughly north-south and divided into eastern and western branches (Tiercelin and Lezzar, 2002). Today, more than 35 tectonic lakes lie within these depressions, either within structural basins or as caldera lakes. Within the eastern branch of the EARS, lakes are generally small and < 50 m deep, whereas the western branch contains several large, deep lakes including Lake Tanganyika and Lake Malawi, with maximum depths of 1470 and 770 m, respectively (Tiercelin and Lezzar, 2002). The basin-fill sedimentary successions include strata of numerous paleolakes of varying sizes and depths that have ceased to exist as a result of climatic change or tectonic activity (Renaut et al., 1999; Tiercelin and Lezzar, 2002).

Kenya's Baringo Basin lies within the eastern branch of the EARS, between 0°15′ and 0°45′N. Together, the Baringo (east) and Kerio (west) basins (Fig. 1C) comprise the oldest deep rift basins of the central Kenya Rift (Tiercelin and Lezzar, 2002). The basins, both east-facing half-grabens, are separated by the uplifted Tugen Hills fault block with the Baringo Basin bounded on the west by the Saimo Fault (Chapman, 1971; Chapman et al., 1978; Martyn, 1969) (Fig. 1B and C). Two modern lakes occupy the inner rift floor of the present-day basin: Lake Baringo (fresh) to the north and Lake Bogoria (saline/alkaline) in a sub-basin to the south (Fig. 1B) (De Cort et al., 2018; Oduor et al., 2003; Okech et al., 2019; Owen et al., 2004; Renaut and Tiercelin, 1994; Tiercelin et al., 1987).

The Baringo Basin is estimated to be filled with up to 7 km of volcanic and sedimentary deposits (Chapman et al., 1978; Hautot et al., 2000; Le Turdu et al., 1995). The basin infill is composed mainly of fluvio-lacustrine deposits of middle Miocene to Pleistocene age, which crop out extensively along the eastern flanks of the Tugen Hills (Fig. 1C) (Hill, 1999; Kingston et al., 2007; Owen and Renaut, 2000; Renaut et al., 1999; Tiercelin et al., 2012). These sediments are significant in part because they form a near continuous stratigraphic succession through a time interval not well represented elsewhere in Africa (Hill, 1999) and they have yielded abundant and diverse faunal assemblages including early catarrhine and later hominin specimens (Hill, 1995, 1985). Sedimentary units are interbedded with volcanic units, including tuffs and lava flows (Chapman et al., 1978; Chapman and Brook, 1978; Deino et al., this issue).

The Neogene history of the Baringo Basin includes the development

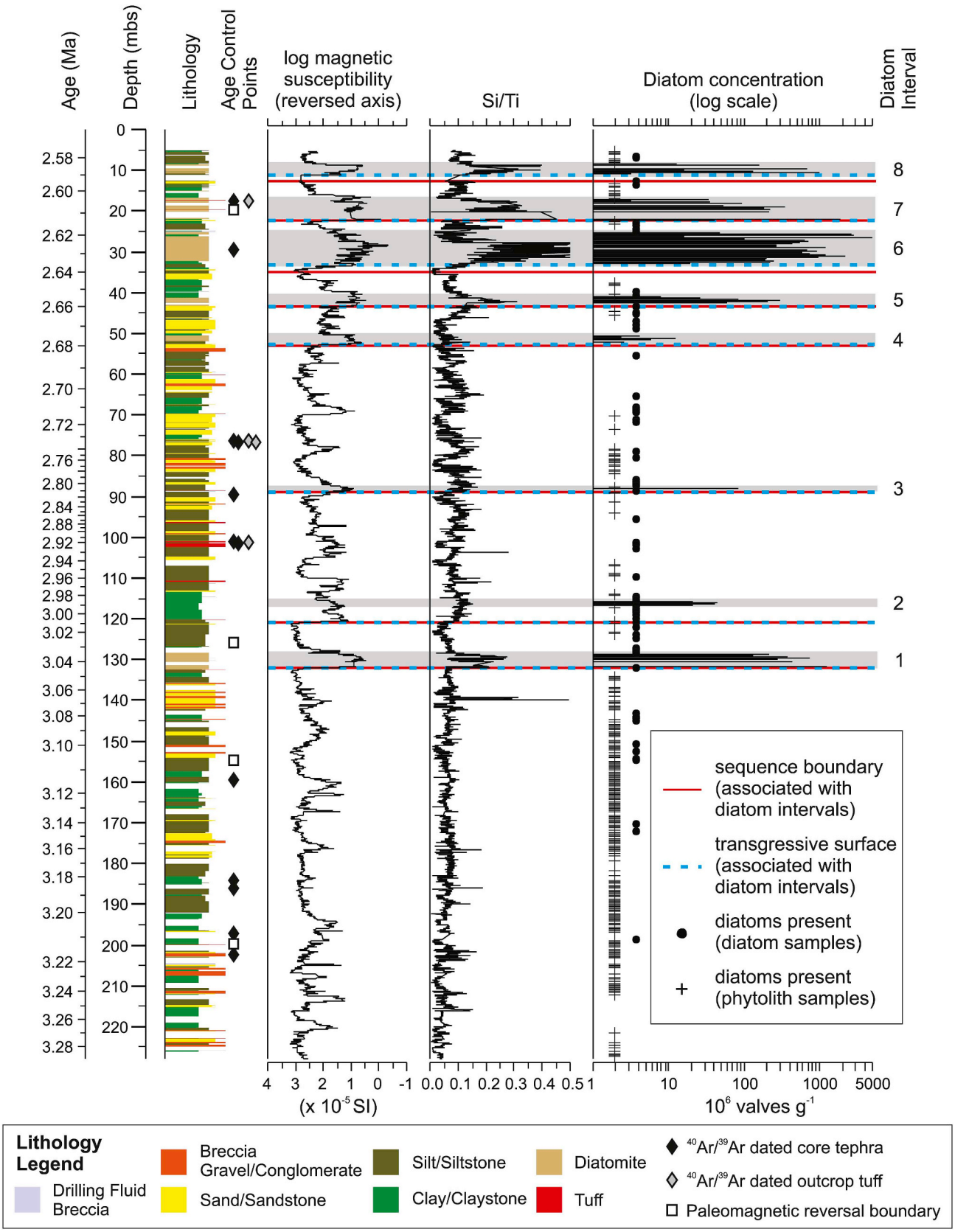

(caption on next page)

Fig. 2. BTB13-1A generalized lithology (Cohen et al., 2016), age control points (Deino et al., this issue), magnetic susceptibility (log MS [x 10^{-5} SI]; 25-pt running average), Si/Ti ratio, and diatom concentration (10^6 valves g^{-1}). Note that the log MS axis is reversed and diatom concentrations are plotted on a log scale. Scaling of the Si/Ti data resulted in high values found in some diatom intervals being cut-off. Filled circles indicate samples where diatoms were observed in very low abundances. Crosses indicate samples where diatoms were observed in samples processed for phytolith analysis, which concentrates microfossils. Shaded bars and corresponding numbers correspond to diatom intervals described in the text. Diatoms found in Interval 4 have been altered by diagenetic processes. Sequence boundaries and transgressive surfaces (Scott et al., this issue) are indicated by solid red and dashed blue lines respectively; some are co-planar. Only boundaries/surfaces that are associated with diatom intervals are plotted here. (For interpretation of the references to colour in this figure legend, the reader is referred to the Web version of this article.)

Table 1
Median values of log MS (x 10^{-5} SI), Si/Ti (XRF), diatom concentration (valves g^{-1}), and ringleiste relative abundance (%) for numbered diatom intervals, an unnamed interval of very low diatom abundance, upper part of core (5.26–132.12 mbs), and entire core.

Diatom Interval (core depth)	median log MS (x 10^{-5} SI)	median Si/Ti	median valve concentration (valves g^{-1})	median ringleiste relative abundance (%)
Interval 8 (8.56–10.95 mbs)	1.04	0.240	1.30×10^8	1.12
Interval 7 (17.08–22.17 mbs)	0.85	0.264	9.24×10^7	8.47
Interval 6 (25.23–32.91 mbs)	0.85	0.219	5.85×10^8	0.51
Interval 5 (40.98–42.55 mbs)	0.95	0.197	7.08×10^7	3.78
Interval 4 (50.67–52.29 mbs)	1.00	0.054	2.99×10^6	0.00
BTB13A-1A-24Q1&2 (68.06–69.37 mbs)	1.30	0.093	–	–
Interval 3 (88.14 mbs)	1.08	0.084	8.24×10^7	54.45
Interval 2 (115.64–116.63 mbs)	1.61	0.124	3.09×10^7	50.82
Interval 1 (128.73–131.58 mbs)	0.70	0.179	3.69×10^8	9.07
entire core	2.45	0.069	–	–
5.26–132.12 mbs	2.13	0.085	–	–

of multiple paleolakes (Owen, 1981; Owen and Renaut, 2000; Renaut et al., 1999), with a progressive eastward shift in the basin depocenter (Tiercelin and Lezzar, 2002). During the Middle to Late Miocene, major lacustrine facies in the Ngorora Formation, Mpesida Beds, and Lukeino Formation of the Tugen Hills succession indicate major freshwater lake systems periodically occupied the Baringo Basin (Chapman, 1971; Hill et al., 1986; Martyn, 1969; Kingston et al., 2002; Owen and Renaut, 2000). Lake basins were continually disrupted by major volcanic pulses that led to the deposition of extensive trachyte, phonolite, and basalt flows intercalated with lacustrine sediments. The Chemeron Formation, first described by McCall et al. (1967), lies disconformably above the Kaparaina Basalt Formation and dates from ~5.3 to 1.6 Ma (Chapman and Brook, 1978; Deino et al., 2002; Deino and Hill, 2002). Diatomites within the upper part of the Chemeron Formation indicate repeated lake transgressions and regressions during this time (Kingston et al., 2007). Subsequent to a ~1 Myr unconformity above the Chemeron Formation, the Middle Pleistocene (~500 ka) Kapthurin Formation comprises fluvial, alluvial, and lacustrine sediments eastward of the Chemeron Formation outcrops (Hill et al., 1986). By ~200 ka, only a small lake remained at the northern end of the basin, an area occupied today by modern Lake Baringo (Renaut et al., 2000; Tiercelin and Lezzar, 2002).

3. Methods

3.1. Diatom analysis

We examined the entire 228-m BTB13-1A core for the presence of diatoms at intervals of approximately 32 cm, or ~400 to 1500 years based on the age model of the core (Deino et al., this issue). Details of core collection can be found in Cohen et al. (2016) and Kingston et al. (this issue). Sample preparation followed standard procedures (Battarbee et al., 2001). Approximately 0.1 g of dry sediment was digested in 35% H_2O_2 to remove residual organic matter. When necessary, samples were mechanically agitated to disaggregate sediment. Samples were rinsed at least four times with reverse osmosis filtered water to remove the H_2O_2. Next, a known quantity of polystyrene microspheres was added to each sample. Samples were then dried onto cover slips and mounted onto microscope slides with Naphrax. Slides were examined using a Leica DM2500 transmitted light microscope at 400–1000x magnification. Diatoms were noted as absent from a sample if no valves or valve fragments were found within two transects examined at 400x. When present, diatom abundance, composition, and preservation were recorded. The presence of diatoms was also noted in slides prepared for phytolith analysis (Yost et al., this issue). Diatom extracts from a representative selection of samples from diatom-rich intervals were mounted on aluminum stubs, sputter coated with gold, and imaged on a TESCAN Vega 3 SEM in high-vacuum mode at 10kV.

Where diatom abundance was sufficient for quantitative analysis, diatoms were identified to species level and counted at 1000x magnification using differential interference contrast (DIC). Identification was based on reference to the Diatoms of North America Taxon Identification Guide (Spaulding et al., 2018), Krammer and Lange-Bertalot (1991, 1986), Gasse (1980), and Houk (2003). For most samples, a minimum of 300 valves were counted. In four samples where diatom abundance was low, samples were counted to a minimum of 100 valves. In addition to valves, separate counts were made of ringleistes and microspheres. A ringleiste is a feature of the valve found in *Aulacoseira* and related ancient genera. It is an unperforated thickened ledge of silica that projects into the interior of the cylindrical valve; because of its robustness, it is typically the last part of the valve to dissolve, leaving behind a ring of silica. Although ringleistes are usually not diagnostic for species-level identification, only one ringleiste is produced per valve; thus, their preservation in our samples provides evidence of the presence of an *Aulacoseira* valve. When calculating relative abundances of diatom species, we used the sum of intact valves and ringleistes in the denominator. As a result, when the percentage of ringleistes is high, the relative abundance of *Aulacoseira* identified to species level is biased (too low) due to our inability to associate ringleistes with a particular taxon. We interpreted the percentage of ringleistes as an indicator of degree of diatom dissolution. Microsphere counts were used to estimate diatom concentration (per gram of sediment) based on the addition of a known quantity of the microspheres to the sample prior to mounting on the slide. We included both valves and ringleistes in our diatom concentration calculations.

3.2. Other environmental indicators

Magnetic susceptibility (MS) was measured using a multisensor core

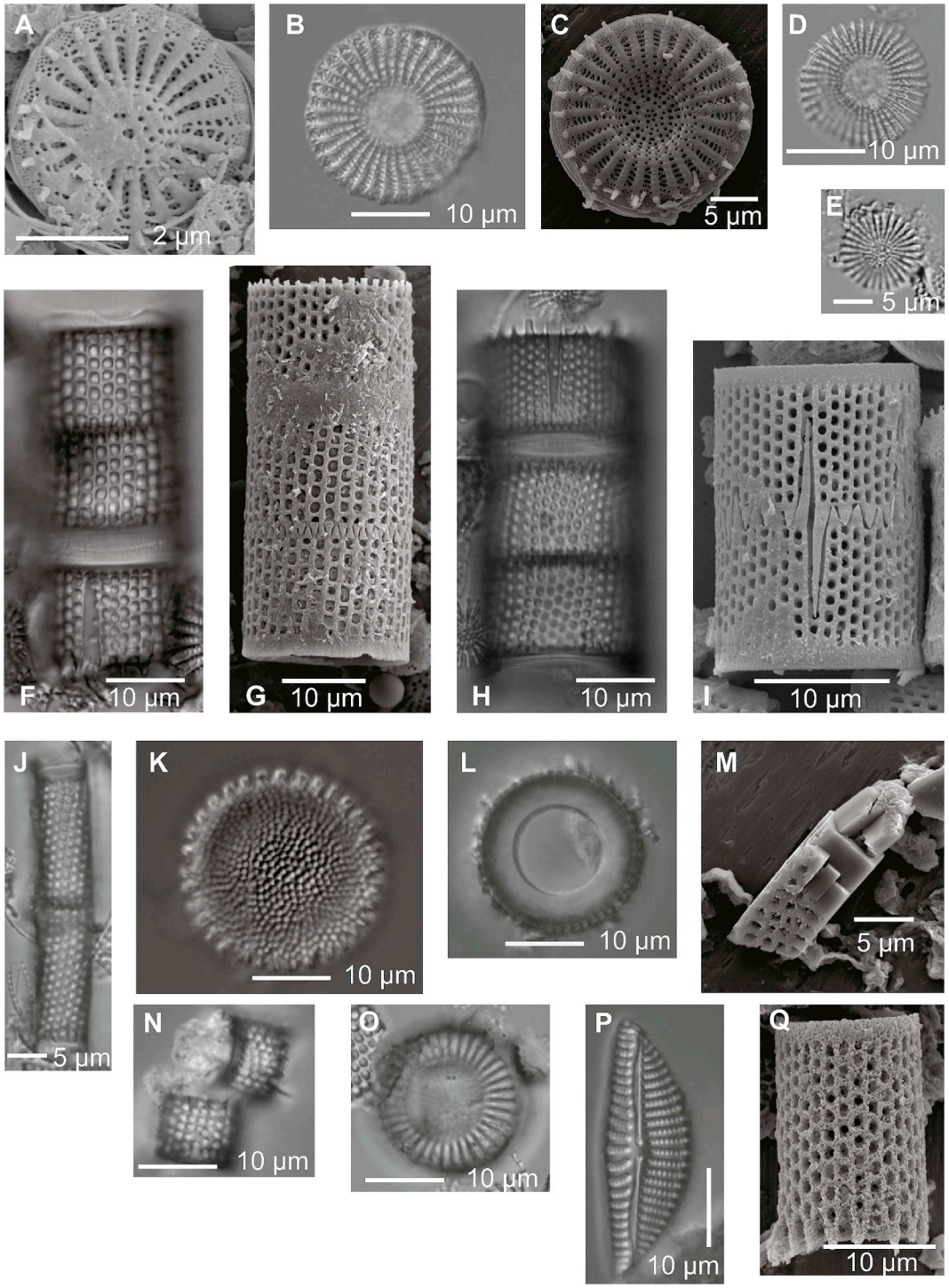

Fig. 3. Light and scanning electron micrographs of dominant taxa found in the BTB13-1A diatomites. A–B) *Stephanodiscus* cf. *subtransylvanicus* v. *minutula* (robust form); C–D) *Stephanodiscus* cf. *subtransylvanicus* v. *minutula* (fine form); E) *Stephanodiscus* sp. 1; F–G) *Aulacoseira granulata* v. *valida*; H–I) *Aulacoseira* sp. 1; J) *Aulacoseira granulata*; K) *Aulacoseira* cf. *agassizii* (valve view); L) *Aulacoseira* ringleiste; M) altered *Aulacoseira* valve from Diatom Interval 4; N) *Aulacoseira* sp. 2; O) *Cyclotella meneghiniana*; P) *Encyonema* cf. *muelleri*; Q) corroded *Aulacoseira* valve.

logger (Geotek MSCL-XYZ) on a split core at 0.5 cm increments and plotted with a 25-point running mean smooth. Elemental concentrations of the sediments (including Si and Ti) were measured by continuous X-ray fluorescence (XRF) scanning of the core at 1-cm resolution. Phytolith samples were prepared using a modified version of the wet oxidation and heavy liquid density separation method described in Piperno (2006), which removes detrital minerals in addition to organic materials. The additional processing of phytolith samples revealed the presence of diatoms in samples in which their concentration was too low to routinely detect under standard diatom processing. Counts of sponge spicules and spherasters were made on phytolith samples. Mineralogy of the sediments was determined by powder X-ray diffraction (XRD) using Panalytical X'pert Pro MPD. The sedimentological analysis of the core was completed by visual and tactile examination of the archive half of the core. Further details on methods of analysis of the same core can be found in Cohen et al.

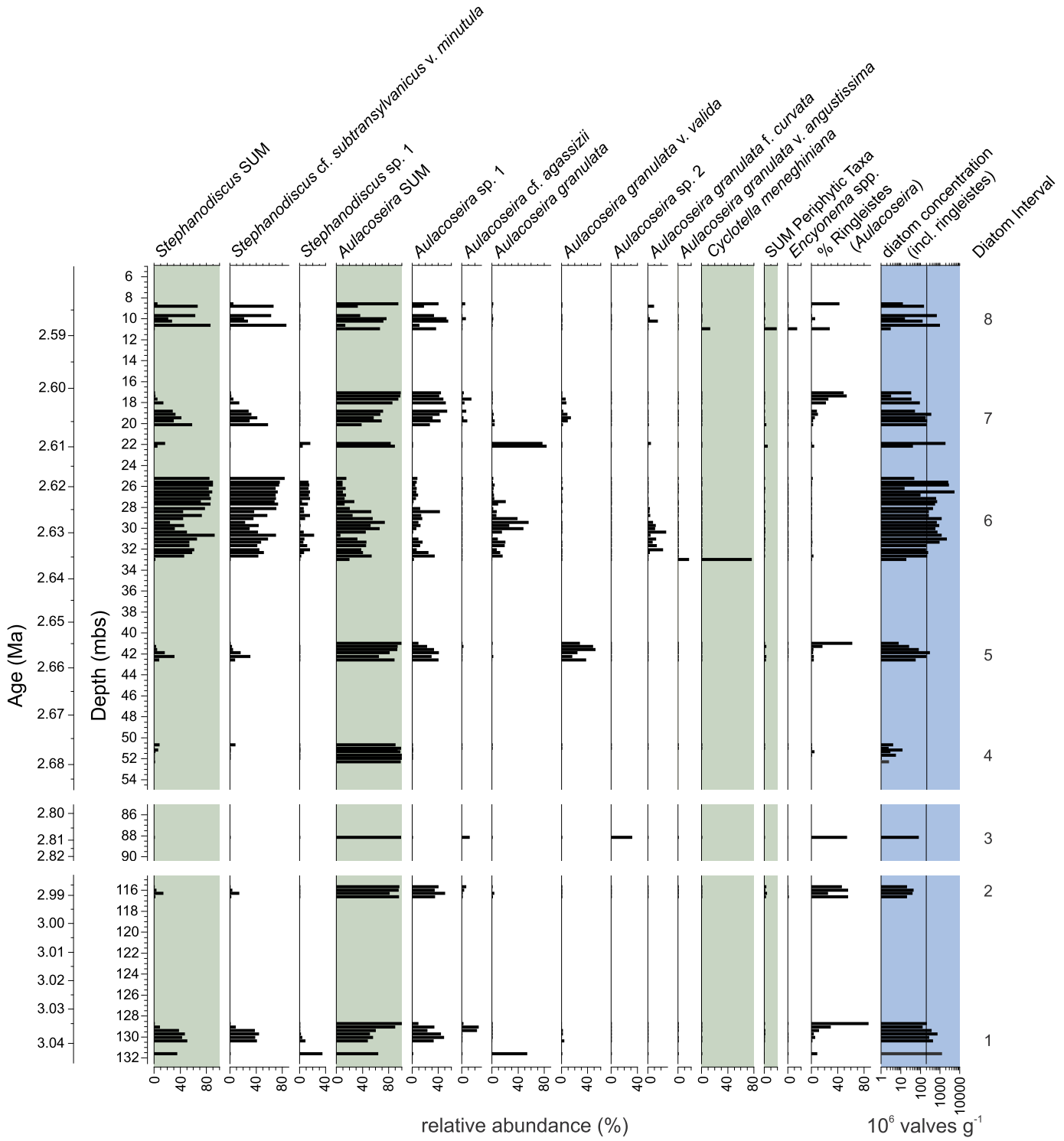

Fig. 4. Diatom stratigraphy of select individual taxa and groups from the upper 132 m of BTB13-1A. Panels shaded in green indicate summed taxa or individual species not represented in any sum. Diatom relative abundance (%) and diatom concentration (valves g^{-1}) are plotted against depth. A secondary age axis is also provided. The stratigraphy is divided into three units encompassing the eight diatom-bearing intervals to account for large sections of the core where diatoms are not found in abundance. Vertical reference line in diatom concentration panel corresponds to median concentration (1.97×10^8 valves g^{-1}). Numbers on right correspond to diatom intervals described in the text. (For interpretation of the references to colour in this figure legend, the reader is referred to the Web version of this article.)

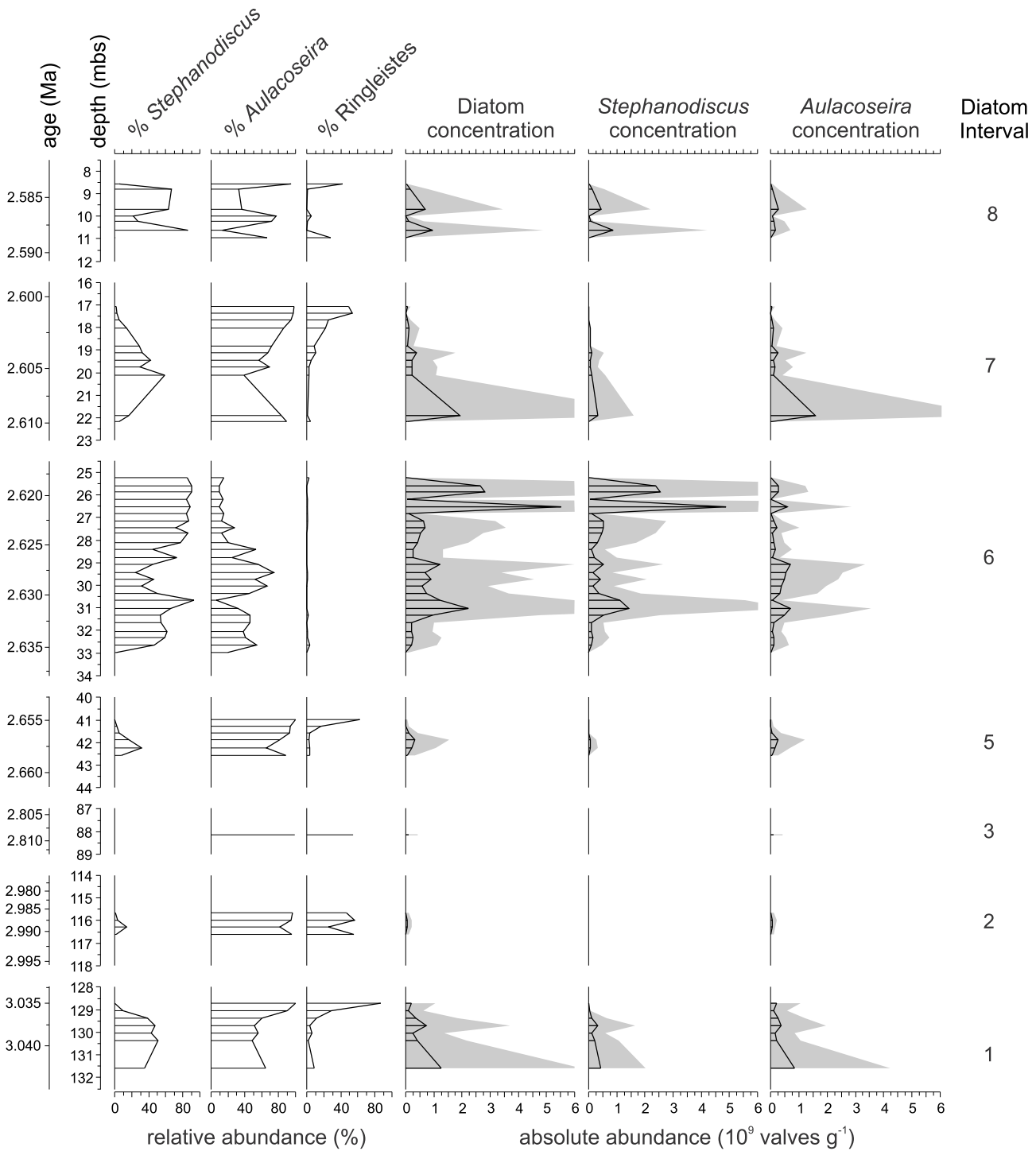

Fig. 5. Comparison of relative and absolute abundance of *Stephanodiscus* and *Aulacoseira.* Absolute abundances are given in valves g^{-1} and calculated from diatom concentrations (including ringleistes). Grey silhouette curves represent 5x exaggeration. High values of ringleiste relative abundance (%) indicate samples with more severe dissolution, where absolute abundance is controlled primarily by preservation. Diatom Interval 4, which featured chemically altered diatoms, is not plotted here.

(2016) (MS), Stockhecke et al. (this issue) (XRF), Yost et al. (this issue) (phytoliths and sponges), Minkara et al. (this issue) (XRD), and Scott et al. (this issue) (sedimentology).

3.3. Core chronology

Deino et al., this issue present a Bayesian stratigraphic age model of the core using control points derived from $^{40}Ar/^{39}Ar$ dating, tephrostratigraphy of tuffaceous units, and paleomagnetic reversal stratigraphy. The distribution of age control points used in the model is shown in Fig. 2.

4. Results

4.1. Diatom presence/absence

We observed diatoms in 141 (23%) of 612 samples processed for diatoms. Of these, only 68 samples (11%) contained diatoms abundant

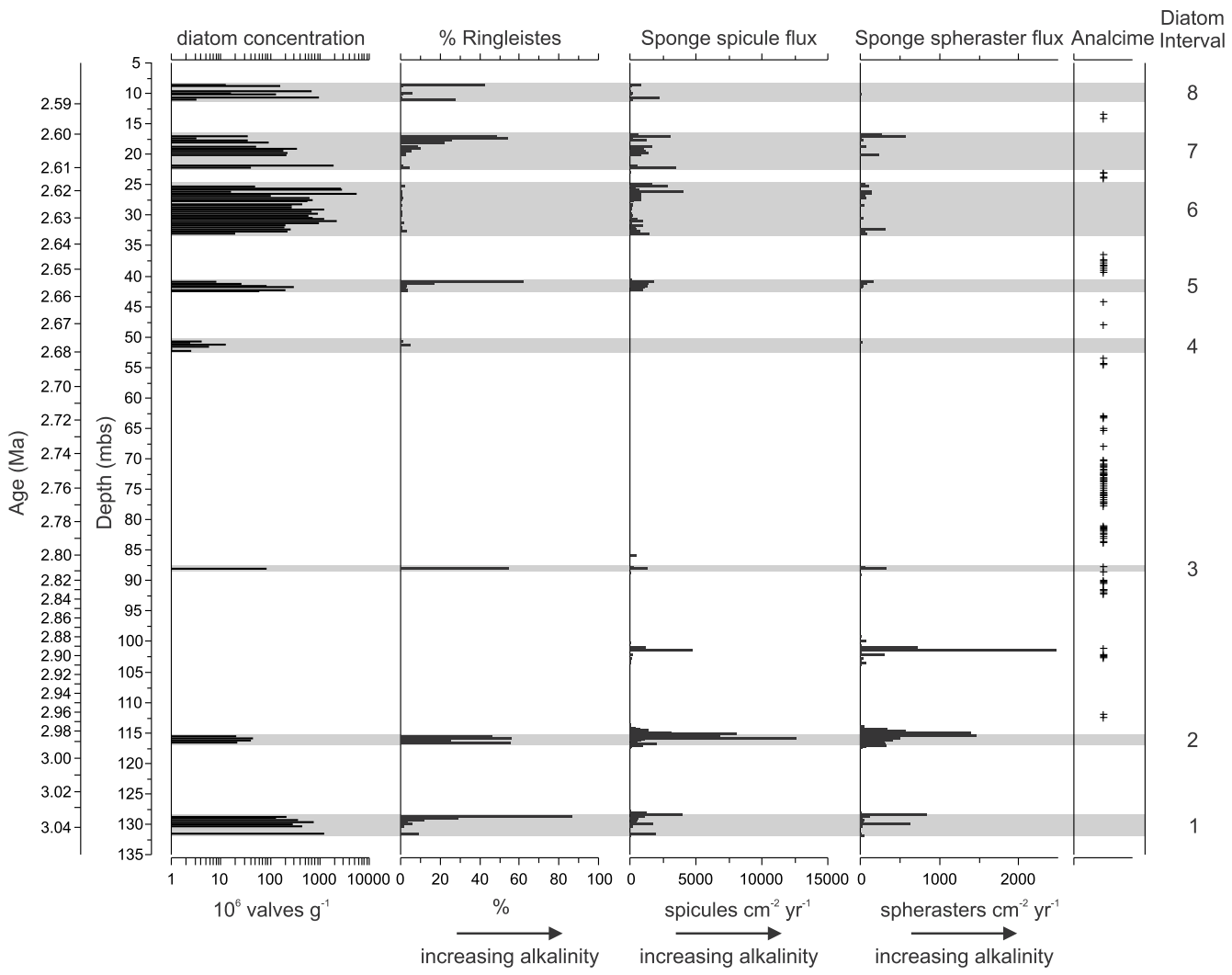

Fig. 6. Diatom dissolution and alkalinity indicators for BTB13-1A. Biogenic silica readily dissolves when pH > 9. As the most robust structural feature of heavily silicified *Aulacoseira* valves, ringleistes are last to disappear from the record. High percentages of ringleistes are an indicator of increased alkalinity. Sponge spicule and spheraster flux also reflects increased alkalinity (Yost et al., this issue). Also plotted is the presence of the zeolite analcime, an indicator of saline alkaline lake or groundwater (Minkara et al., this issue). Shaded bars correspond to diatom intervals discussed in the text.

enough for quantitative analysis. These diatom-rich samples are distributed into eight intervals within the upper 132 m of BTB13-1A (Fig. 2). One of the intervals (Interval 4; 50.67–52.29 mbs) contains poorly preserved diatoms at relatively low abundances. This interval was counted to determine diatom concentration but poor preservation limited identifications to genus level. Examination of these samples by scanning electron microscope revealed the diatom valves to be altered by devitrification. Diatoms were also observed in very low abundances in an additional 241 samples prepared for phytolith analysis (Yost et al., this issue) (Fig. 2). Subsequent discussion of diatom observations is based on the samples processed for diatoms.

The paucity of diatoms in much of the core was not unexpected as we examined all samples regardless of lithology, and diatoms typically do not accumulate in substantial concentrations in sediments deposited in high-energy or non-lacustrine environments that characterize sections of the core. Although freshwater diatoms live in a variety of aquatic environments, their remains are infrequently found in abundance in deltaic or fluvial settings due to siliciclastic dilution and sediment redistribution. In many cases, diatoms found in samples with very low diatom abundance are characterized by features indicating poor preservation, including fragmentation, dissolution, and apparent post-depositional alteration. Evidence of dissolution of both diatoms and phytoliths in some intervals suggests that diatoms are absent from some lacustrine sediments due to conditions unfavorable to biogenic silica preservation.

Six of the eight diatom intervals (Diatom Intervals 1 and 4–8 in Fig. 2) identified in the upper 132 m of BTB13-1A correspond to units identified as “diatomites” in the initial core description (Cohen et al., 2016). However, the low abundance and poor preservation of diatoms in Diatom Interval 4 indicate that it was misclassified in the initial core description. The other two intervals (Diatom Intervals 2 and 3) are characterized in that description as silt, silty clay, and clay. The eight intervals are found unevenly distributed in the core. Five intervals are located in the upper 52 m of the core. An interval at 88.14 m below surface (mbs) is represented by a single sample and the oldest two intervals are found between 115 and 132 mbs. Samples with very low diatom abundance (insufficient for counts) were found: (i) as transitional zones adjacent to and likely as extensions of intervals of higher abundance (ii) as separate intervals (i.e., multiple adjacent samples) of poor preservation; or (iii) as solitary samples.

The concentration of diatom valves (valves g^{-1}) across all counted intervals varied over three orders of magnitude (10^6–10^9 valves g^{-1}) (Westover and Stone, 2019). Diatom concentration reflects several processes including: (i) diatom production; (ii) preservation of valves, which may be lost by dissolution and/or fragmentation; and (iii) dilution by detrital components of the sediment. Hence diatom

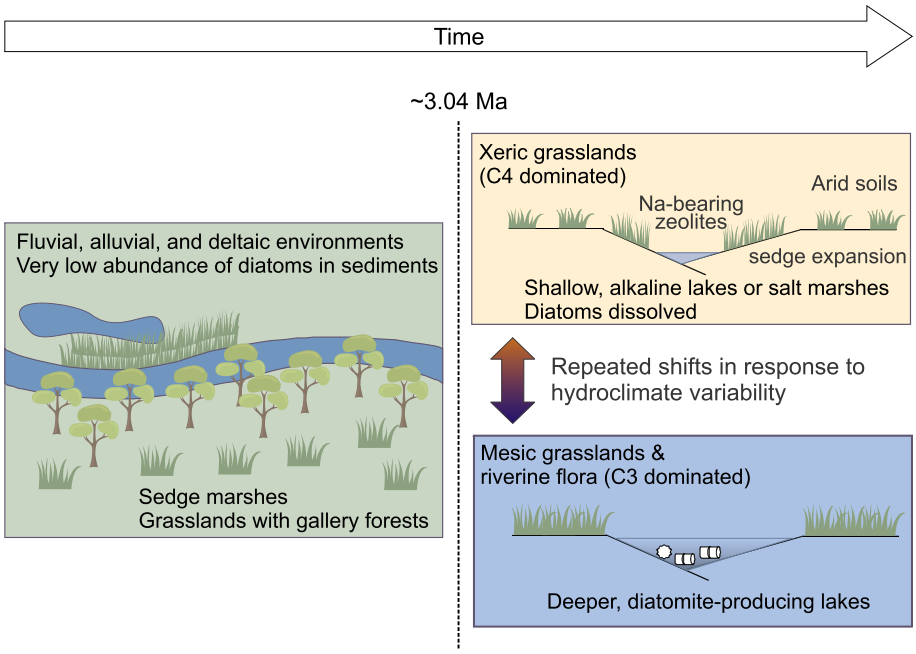

Fig. 7. Simplified model of depositional environments as related to the presence of diatoms in the BTB13-1A core. Prior to ~3.04 Ma, fluvial, alluvial plain and lake-marginal environments dominated. When freshwater diatoms were preserved before 3.04 Ma, their numbers were diluted by sedimentation of detrital grains. After ~3.04 Ma, a deep, freshwater lake system developed leading to the deposition of diatomite. Significant fluctuations in lake conditions followed, with periods of dissolution of diatoms and other siliceous microfossils associated with increased salinity and alkalinity of lake water, zeolite precipitation, and sedge expansion.

concentration is not a unique indicator of a single process and inferences should be supported by additional lines of evidence.

Diatom-bearing units correlate well to low magnetic susceptibility (MS) of core sediments (Fig. 2) (Cohen et al., 2016). Magnetic susceptibility is a measure of induced magnetization of sediments and reflects the concentration of magnetic minerals. Variation in this sediment property may reflect relative proportions of weakly or non-magnetic biogenic sediments and detrital minerals, as is the case here. Diatom-rich units have uniformly low magnetic susceptibilities (reported as volume magnetic susceptibility [x 10^{-5} SI]) with median log MS values from 0.70 to 1.61 (Table 1). The lowest sustained MS values generally occur within diatomites, attributable to their high proportion of biogenic silica. There are two intervals of relatively low MS (Interval 4 and an unnamed interval from 68.06–69.37 mbs) where diatoms are present but in very low abundances. We also identified one diatom-bearing interval (Interval 2) that corresponds to moderately low MS (median log MS = 1.61). Median log MS for the entire core was 2.45 (2.13 for the upper 132 m). There are five intervals where diatom concentrations exceeded the median (1.97×10^8 valves g^{-1}) in at least one sample. In these intervals, median log MS values range from 0.70 to 1.04 (Table 1). In four other diatom-bearing units, median log MS values range from 1.00 to 1.61.

Si/Ti has been used as an indicator of the abundance of biogenic silica (BSi) in lake sediments based on correlations between Si/Ti and BSi determined by chemical digestion (Brown et al., 2007; Johnson et al., 2011). A similar relationship is observed in the BTB13-1A core between diatom concentration and Si/Ti (Fig. 2), with elevated Si/Ti corresponding to high diatom concentrations.

4.2. Diatom taxonomy

The diatom record of the BTB13-1A core is dominated by species belonging to the planktonic genera *Stephanodiscus* and *Aulacoseira* (Figs. 3 and 4) (Westover and Stone, 2019). This was the case in samples of both high and very low diatom abundance. Two species of *Stephanodiscus* are recognized. The dominant species may be *Stephanodiscus subtransylvanicus* v. *minutula* Gasse 1980, which was originally described from Pliocene deposits of Ethiopia (Gasse, 1980). The BTB taxon appears to show some morphological variation associated with degree of silicification (Fig. 3A–D). The identity of the second species or its affinity has not yet been determined (hereafter referred to as *Stephanodiscus* sp. 1), but it is characterized as a distinct form because its average valve diameter is smaller and it is more lightly silicified than *S. subtransylvanicus* v. *minutula* (Fig. 3E).

We identified several species of *Aulacoseira*, including *A. granulata* (Ehrenb.) Simonsen 1979, *A. granulata* v. *valida* (Hustedt) Simonsen 1979, and *A. granulata* f. *curvata* (Hustedt) Simonsen 1979. Another *Aulacoseira* species was observed but remains unidentified; it may represent an undescribed species (hereafter referred to as *Aulacoseira* sp. 1) (Fig. 3H–I). *Aulacoseira* sp. 1 appears most similar to *A. muzzanensis* (F. Meister) Krammer 1991. Both our taxon and *A. muzzanensis* overlap with *A. granulata* in characteristics of valve structure but, in both, the ratio of mantle height to valve diameter is less than *A. granulata*. We have also separately counted a similar taxon characterized by a large diameter and very short mantle such that it was most often observed in valve or top view (most *Aulacoseira* are observed in girdle or side view) (Fig. 3K). This taxon may be *A. agassizii* (Ostenfeld) Simonsen 1979, *Aulacoseira* sp. 1, or an as yet undescribed species. It is hereafter referred to as *A.* cf. *agassizii*. A third, unidentified species of *Aulacoseira* (hereafter referred to as *Aulacoseira* sp. 2) was observed in a single sample only. It likely also belongs within the *A. granulata* complex and differs from *Aulacoseira* sp. 1 by its smaller size range and larger areolae (Fig. 3N).

Another planktonic taxon, *Cyclotella meneghiniana* Kützing 1844, was observed in significant proportions in single samples found at the bases of two diatom-bearing intervals. Several oligotrophic planktonic species (*Lindavia* cf. *ocellata, Lindavia* cf. *comensis,* and *Discostella* cf. *stelligera*) were observed in multiple samples from 127–128 mbs and 143–145 mbs. However, counts were not made of these samples because of very low diatom concentrations and no paleoenvironmental inferences are drawn as a result. Periphytic taxa (most commonly species of *Staurosira, Staurosirella, Encyonema, Cocconeis and Amphora*) were usually present at low relative abundances (mean = 1.2%; median = 0.7%).

4.3. Characteristics of diatom-bearing intervals

4.3.1. Diatom Interval 1

This interval is represented by seven samples between 131.58 and 128.73 mbs (3.043–3.035 Ma), with a gap (unrecovered sediments) between 131.56 and 130.58 mbs. At the base of this interval (131.58 mbs), diatom concentrations are very high (1.25×10^9 valves

g^{-1}; 92nd percentile) despite some dissolution as indicated by the presence of *Aulacoseira* ringleistes. *Aulacoseira granulata* dominated this initial assemblage (64%), with *Stephanodiscus* sp. 1 comprising most of the remaining assemblage. Above the missing section, the assemblage is composed of *Stephanodiscus* cf. *subtransylvanicus* v. *minutula, Aulacoseira* sp.1, and *Aulacoseira cf. agassizii*. The relative abundances of the two genera are each close to 50% of the assemblage until 129.38 mbs, when *S.* cf. *subtransylvanicus* v. *minutula* falls to 38%. Concentrations from 130.37 to 129.38 mbs are less than the basal sample but remain relatively high (64th–83rd percentile). The upper part of Interval 1 (129.06–128.73 mbs) is characterized by the diminishing presence of *Stephanodiscus* and its complete absence at the top of the interval. This trend may reflect preferential preservation of *Aulacoseira*, as indicated by an increasing relative abundance of ringleistes, which reaches 87% at the top of the interval (128.73 mbs), and decreasing valve concentration (2.11×10^8 valves g^{-1}). Diatoms were found in very low abundances (uncounted) extending ~1.5 m above this interval.

4.3.2. Diatom Interval 2

Interval 2 is represented by four samples from 116.63 to 115.64 mbs (2.991–2.986 Ma). This interval is characterized by a higher concentration of detrital grains than other intervals, as evidenced by lithology (silty clay), relatively high MS (median log MS = 1.61), and relatively low Si/Ti (Table 1; Fig. 2). Low diatom concentrations (median = 3.09×10^7 valves g^{-1}; 20th–31st percentile) are likely driven more by dissolution (25–56% ringleistes) than dilution. This interval is characterized by a low average sedimentation rate (0.02 cm yr^{-1}) compared to other diatom-bearing intervals (0.04–0.06 cm yr^{-1}).

The assemblage is dominated by *Aulacoseira* sp. 1, with relative abundances of *S.* cf. *subtransylvanicus* v. *minutula* of 1–14%. It is likely that the assemblage has been biased as a result of preferential preservation of the more heavily silicified *Aulacoseira* valves. This assemblage also features higher percentages of periphytic taxa relative to other intervals, although values are still low (1–4%). Diatoms were observed in very low abundance (and poorly preserved) extending 2 m below and ~1 m above this interval.

4.3.3. Diatom Interval 3

Interval 3 is represented by a single sample (88.14 mbs; 2.808 Ma), although diatoms were found in very low abundance extending ~2 m above and 0.33 m below this sample. The sample features higher diatom concentrations than Interval 2 (8.24×10^7 valves g^{-1}; 30th percentile), but is also characterized by dissolution and dilution by detrital components; it is described lithologically as silt. Although MS is relatively low at this depth (log MS = 1.08), light microscopy and a low Si/Ti indicate increased detrital sedimentation relative to the true diatomites observed in other parts of the core. The assemblage is composed almost entirely of *Aulacoseira,* including *A. cf. agassizii* and *Aulacoseira* sp. 2, with less than 1% *Stephanodiscus.* Although there may be some preservation bias, *Aulacoseira* is likely to have been the dominant taxon.

4.3.4. Diatom Interval 4

Interval 4 comprises seven samples from 52.29 to 50.67 mbs (2.679–2.676 Ma). Although it resembles other diatomite units macroscopically and was initially described as a diatomite (Cohen et al., 2016), diatoms are present in low abundances (median = 2.99×10^6 valves g^{-1}) and show evidence of devitrification (Fig. 3M). Due to mineralization of the diatoms, we were unable to identify most valves to species. *Aulacoseira* dominates the interval (91–100%), which is also characterized by few ringleistes. *Stephanodiscus* reaches a maximum of 8% at the top of the interval. Although MS values for this interval are similar to other diatom-bearing intervals, its Si/Ti ratio is low (Table 1), reflecting a low abundance of biogenic silica.

4.3.5. Diatom Interval 5

Interval 5 is represented by six samples from 42.55 to 40.98 mbs (2.658–2.655 Ma). As measured by % ringleistes (2–62%), diatom preservation in this interval is generally good, however examination of these samples by SEM revealed evidence of valve corrosion (Fig. 3Q). Diatom concentrations increase (peak at 3.03×10^8 valves g^{-1}; 65th percentile) and then decrease to a very low concentration (8.02×10^6 valves g^{-1}) at the top of this interval. Interval 5 is dominated by two *Aulacoseira* species: *Aulacoseira granulata* v. *valida* and *Aulacoseira* sp. 1. *Stephanodiscus* cf. *subtransylvanicus* v. *minutula* is also present, with a maximum abundance of 31% at 42.24 mbs. The top of the interval (40.98 mbs) is severely dissolved (62% ringleistes). Diatoms were observed in very low abundances from ~1 m below to 0.34 m above this interval.

4.3.6. Diatom Interval 6

Interval 6 is represented by 25 samples over nearly 8 m of core section (32.97–25.23 mbs). This interval represents the most persistent period of diatom accumulation in the core, spanning ~17,000 years from 2.635 to 2.618 Ma. Preservation is excellent and diatom concentrations are typically very high (median = 5.85×10^8 valves g^{-1}) with only five samples with concentrations below the 50th percentile for all counted samples. Concentrations are lowest near the bottom and top of the interval, with very low abundances of diatoms extending 0.8 m above the interval. The basal sample of this interval (32.97 mbs) features low concentrations of a distinct assemblage composed of 77% *Cyclotella meneghiniana*, 20% *Aulacoseira* (possibly *A. granulata* v. *angustissima* (O. Müller) Simonsen 1979), and 2% *Stephanodiscus*. This assemblage was replaced by the typical *Stephanodiscus* and *Aulacoseira* assemblage. *Stephanodiscus* is more abundant (50–92%) than *Aulacoseira* from 32.32 to 30.04 mbs, above which *Aulacoseira* dominates (52–74%). From 28.13 mbs to the top of the interval, *Stephanodiscus* again dominates the assemblage (44–90%). The assemblage includes both species of *Stephanodiscus*, although *S.* cf. *subtransylvanicus* v. *minutula* is more abundant. The *Aulacoseira* taxa comprise *A. granulata*, *Aulacoseira* sp. 1, and *A. granulata* f. *curvata.* Where *Aulacoseira* species dominate in the middle of the interval, *A. granulata* is more abundant. An unidentified species of *Nitzschia* was observed from 32.05 to 27.68 mbs in low relative abundances (< 2.5%). *Nitzschia* is a diverse genus that includes both planktonic and periphytic forms. Planktonic species are typically very long and narrow, compared to typically smaller periphytic species. The morphology of the taxon suggests it is most likely planktonic.

4.3.7. Diatom Interval 7

Interval 7 is represented by 11 samples from 22.17 to 17.08 mbs (2.610–2.601 Ma). There are two gaps in recovery in this section, from 21.84 to 20.25 mbs and 18.81 to 18.02 mbs. This diatomite features high concentrations (median = 2.20×10^8 valves g^{-1}) and good preservation (1–10% ringleistes) from 21.89 to 19.12 mbs, and low concentrations (median = 3.57×10^7 valves g^{-1}) and poorer preservation (8–54% ringleistes) from 18.82 to 17.08 mbs. The basal sample (22.17 mbs) is composed of 84% *A. granulata* with 5% *Stephanodiscus* sp. 1 and 5% periphytic taxa (greater than is typical in the core). This sample also features low concentrations (4.10×10^7 valves g^{-1}) and evidence of moderate dissolution (4% ringleistes). Above 20.25 mbs, the assemblage shifts to co-dominance by *S.* cf. *subtransylvanicus* v. *minutula* and *Aulacoseira* sp. 1. *Stephanodiscus* is more abundant at 20.10 mbs, but decreases in relative abundance above this level until it comprises less than 3% of the assemblage at the top of the interval. Strong dissolution in samples between 18.01 and 17.08 mbs suggests the assemblages may be biased by preferential preservation of *Aulacoseira.*

4.3.8. Diatom Interval 8

Interval 8 is represented by seven samples from 10.95 to 8.56 mbs

(2.589–2.584 Ma), with a gap in recovery from 9.70 to 9.02 mbs. There is also a gap in recovery just below this interval from 12.69 to 11.12 mbs, making the true base of the interval uncertain. Diatom preservation is good, except at the bottom and top, where it is poor. The basal assemblage (10.95 mbs) is composed of 67% *Aulacoseira* sp. 1, 13% *C. meneghiniana*, and 19% periphytic taxa (most of which was likely *Encyonema muelleri* (Hustedt) D. G. Mann 1990). The basal sample features very low diatom concentrations (3.15×10^6 valves g^{-1}) and moderately strong dissolution (28% ringleistes). The next sample at 10.63 mbs is dominated by *S.* cf. *subtransylvanicus* v. *minutula* with < 15% *Aulacoseira* (mostly *Aulacoseira* sp. 1). The rest of Interval 8 features alternating dominance between *S.* cf. *subtransylvanicus* v. *minutula* and *Aulacoseira* sp.1. *Aulacoseira granulata* f. *curvata* is present in relative abundances from 0.5 to 15% beginning at 10.24 mbs. Diatom concentration maxima at 10.63 and 9.71 mbs (9.8×10^8 and 6.9×10^8 valves g^{-1}, respectively) correspond to high relative abundances of *Stephanodiscus*. However, high relative abundances of *Stephanodiscus* were also observed in samples with more moderate concentrations. At the top of this interval (8.56 mbs), diatom concentrations are low (1.26×10^7 valves g^{-1}) and dissolution effects are strong (42% ringleistes), preferentially preserving *Aulacoseira*. High log MS (> 2) and low Si/Ti (0.11) at the top of Interval 8 also indicate a higher fraction of detrital minerals.

5. Discussion

5.1. Characteristics of the Baringo paleolakes

The characteristics of the diatom-rich intervals in the BTB13-1A core suggest that these diatomaceous sediments were deposited offshore within relatively deep, freshwater systems that persisted on the landscape for periods ranging from ~3000 to 17,000 years long. Generally, lacustrine diatomites form in mesotrophic to eutrophic systems with sufficient silica (Si) and phosphorus (P) to sustain high diatom production in combination with low allochthonous inputs (Harwood, 2010). The dominant diatom taxa of the BTB13-1A core belong to genera (*Aulacoseira* and *Stephanodiscus*) that require high Si and/or P, which further supports this inference. In an extensive study of diatoms from the modern sediments of Lake Malawi, Owen and Crossley (1992) observed pure diatomaceous ooze forming at water depths < 150 m in the shallow southern basin. They attributed these sediments to lake mixing releasing nutrients (Si and P) that stimulate diatom production combined with minimal clastic inputs. The lack of detrital material in the BTB13-1A diatomites is consistent with deposition having occurred offshore, with limited sediment influx.

In lakes, periphyton inhabit the shallow, sunlit waters of the littoral zone. The transition from periphyton-dominated to plankton-dominated sediments occurs at approximately the depth of penetration of 1% incident light (e.g., Moos et al., 2005), a property that is lake-specific and may vary over time. The relative abundance of littoral species in offshore sediments depends on proximity to the lake margin, littoral zone productivity, and sediment transport processes (Gasse et al., 2002; Wolin and Stone, 2010). The very low percentages of periphyton observed in the diatom-rich intervals of the BTB13-1A core suggest these sediments were deposited some distance from littoral zones. Alternatively, a steep-sided lake basin with limited littoral area, potentially characteristic of structurally complex grabens, could also produce low proportions of periphytic taxa nearer to shore (Stone and Fritz, 2004).

The exclusively planktonic assemblages of the BTB13-1A diatom record limit diatom-based inferences of lake level. By themselves, planktonic diatoms are generally not very sensitive indicators of water depth, because they require only sufficient water depth to remain suspended in the water column and can be abundant in shallow lakes. Attempts to reconstruct water depth using diatom inference models based on in-lake depth transects has shown deep water sediments to be insensitive to lake-level changes due to very high percentages of planktonic taxa (Laird et al., 2010; Laird and Cumming, 2009).

Species of both *Aulacoseira* and *Stephanodiscus* are dominant components of the plankton in both shallow and deep African rift lakes today and in the past, including Lake Malawi (Gasse et al., 2002; Owen and Crossley, 1992; Pilskaln and Johnson, 1991; Stone et al., 2011), Lake Tanganyika (Haberyan and Hecky, 1987), Lake Albert (Evans, 1997; Kilham et al., 1986), Lake Victoria (Gasse et al., 1983; Stager, 1984; Stager and Johnson, 2000; Talling, 1986), Lake Rukwa (Haberyan, 1987), and Pliocene Lake Gadeb (Ethiopia) (Gasse, 1980). However, the consistently low fraction of periphyton is suggestive of moderately deep water. Open-water diatom assemblages from Lake Naivasha (< 10 m) are dominated by *Aulacoseira* but periphytic *Cocconeis* and *Navicula* species make up a significant fraction (Hubble and Harper, 2002). In Lake Baringo today (mean depth = 3 m), the diatom community is dominated by *Aulacoseira*, although periphytic *Cymbella* is also common (Schagerl and Oduor, 2003). In contrast, in the southern basin of Lake Malawi, Haberyan and Mhone (1991) observed that periphytic taxa never comprised more than 2% of the assemblage in offshore plankton tows. Thus, the consistently low fraction of periphyton suggests that the sediments of BTB13-1A were deposited in deeper waters.

Further, if the BTB13-1A assemblages represent more shallow, open-water conditions, close to the transition between periphyton- and plankton-dominated sediments, we would expect to see increases in periphyton during the early stages of regressions before significant increases in alkalinity and pH. For example, the Pleistocene diatom record of Lake Naivasha (Bergner and Trauth, 2004) features distinctly littoral assemblages in addition to highstand planktonic assemblages. In contrast, we only observed dissolution of the planktonic assemblages, suggesting that the lake remained relatively deep even as lake levels fell and alkalinity increased due to evaporative concentration. This observation is supported by the carbon isotope record of fish bones, which indicates exclusively pelagic, deep-water fish both within diatomite intervals and in intervals where diatoms are not preserved (Billingsley et al., this issue).

The scarcity of littoral diatoms and lack of littoral fish observed in the BTB13-1A core during transgression and regression may also indicate rapid expansion and contraction of the lake, and/or a rapid change in lake conditions (e.g., pH). For comparison, lake-level fluctuations of up to 100 m in less than 100 years have been documented in paleolake Suguta (Kenya) during the African Humid Period (Junginger and Trauth, 2013). The term amplifier lake has been used to describe certain rift lakes in East Africa that have experienced large fluctuations in lake level in response to moderate climate fluctuations (Trauth et al., 2010). The climatic sensitivity of these lakes is explained by basin morphology and contrasts in hydroclimate between high elevations (high precipitation) and low elevations (high evaporation) within the catchment (Olaka et al., 2010; Trauth et al., 2010). The lakes most sensitive to precipitation variability have been identified as those characterized by a distinct graben basin morphology and a relatively humid climate (Olaka et al., 2010).

The dominant species of *Aulacoseira* found in the BTB13-1A core belong to the *Aulacoseira granulata* complex (*A. granulata, A. granulata* v. *valida*, and *Aulacoseira* sp. 1). This species complex is considered a cosmopolitan freshwater group and is commonly reported in shallow lakes, rivers, and marginal regions of larger lakes (Kilham and Kilham, 1975) and is associated with abundant Si and P (Kilham et al., 1986). In the extremely deep modern Lake Malawi and Lake Tanganyika, this group is found in abundance only in relatively shallow areas (< 200 m), where the water column is well mixed and enhanced upwelling supplies abundant nutrients (Haberyan and Mhone, 1991; Owen and Crossley, 1992). *Aulacoseira granulata* reportedly blooms in the highly productive shallow bays of Lake Victoria (maximum depth = 81 m, mean depth = 40 m) but is uncommon in the open lake, which is more strongly stratified (Stager, 1984). Species belonging to

the *Aulacoseira granulata* complex have also been reported from Holocene sediments collected from Lake Victoria (Stager, 1984; Stager and Johnson, 2000) and Lake Albert (Kilham et al., 1986). At present, Lake Albert has an area of 5300 km^2, a maximum depth of 51 m, and a mean depth of 25 m. Kingston et al. (2007), in examining these diatomaceous sediments from outcrop, also concluded that the lakes that produced these diatomites must have been at least 20 to 40 m deep based on the presence of fine laminae indicative of anoxic bottom waters. Accordingly, we infer that the Baringo Basin paleolakes between ~2.68–2.58 Ma and ~3.04–2.98 Ma were moderately deep and typically well mixed during the freshwater phases represented by these diatom-rich stratigraphic intervals.

5.2. Diatom ecology and paleolimnological interpretation

Observational studies as well as growth experiments have provided a robust, general model based in resource ratio theory (Tilman et al., 1982) for understanding the ecological niches of the major planktonic groups including *Aulacoseira* and *Stephanodiscus* (Haberyan and Hecky, 1987; Haberyan and Mhone, 1991; Hecky and Kling, 1987; Kilham, 1990, 1971; 1986, 1984; Kilham et al., 1986, 1996; Kilham and Kilham, 1975; Owen and Crossley, 1992; Pilskaln and Johnson, 1991; Talling, 1986). Variability in the composition of planktonic diatom assemblages is best understood as a response to changing nutrient concentrations, mixing/stratification, and light availability (Kilham et al., 1986; Owen and Crossley, 1992). These factors are, of course, dependent on one another and influenced by climate, basin morphometry, and catchment characteristics. With respect to freshwater lakes in East Africa, Kilham et al. (1986) explained the abundances of a variety of planktonic diatoms (including species of *Aulacoseira* and *Stephanodiscus*) in terms of the relative availability of Si and P, in addition to light. Most planktonic diatoms in these lakes did not appear to respond to nitrogen limitation.

The life history of the typically meroplanktonic *Aulacoseira* differs from many other planktonic diatoms. *Aulacoseira* are chain-forming and many species are heavily silicified relative to other planktonic diatom groups. *Aulacoseira* is favored under a high Si:P ratio (Kilham et al., 1986). In other words, *Aulacoseira* has high requirements for Si, but is a good competitor when P is limiting. Periods of dominance by *Aulacoseira* are produced by enhanced mixing, which creates an upward flux of Si from the hypolimnion as well as the convective mixing required to keep cells suspended. As mixing decreases and nutrient flux diminishes, the heavy *Aulacoseira* chains rapidly sink out of the water column. Thus, *Aulacoseira* blooms are observed under conditions of strong convective mixing, and are replaced by other groups (i.e., *Stephanodiscus*, *Nitzschia,* and cyanophytes) when convective mixing is less intense (Haberyan and Mhone, 1991; Jewson, 1992; Kilham et al., 1986). Because they are associated with deeper mixing, *Aulacoseira* are generally considered good competitors for light (i.e., they do well when light is limiting). When conditions become unfavorable, many *Aulacoseira* species form resting cells that can persist in the sediment until resuspended (typically from shallow areas) in the next growing season (McQuoid and Hobson, 1996; Sicko-Goad et al., 1986).

In contrast, the euplanktonic *Stephanodiscus* is associated with low Si:P ratios (Kilham et al., 1986). Typically, *Stephanodiscus* is a poor competitor for P (requiring moderately high levels), but a good competitor for Si. The contrasting nutrient requirements of diatom taxa are often reflected in patterns of seasonal succession. Under conditions of thermal stratification, the sunlit epilimnion becomes depleted in Si and P due to uptake by diatoms. Conversely, the hypolimnion becomes a reservoir for these nutrients as they are exported by the sedimentation of diatoms. When stratification breaks down (from seasonal winds, for example), the nutrients are resupplied to the epilimnion and trigger blooms. Thus mixing, in particular deep mixing, favors *Aulacoseira* production via re-supply of nutrients and the convection necessary to maintain their position in the photic zone. *Stephanodiscus*, in turn, although requiring some mixing to supply P, is more likely to be associated with weaker or shallower mixing. For example, in Lake Malawi, a distinct seasonal pattern in *Stephanodiscus* and *Aulacoseira* abundance is related to the thermal structure of the lake and depth of mixing (Haberyan and Mhone, 1991; Hecky and Kling, 1987; Kilham et al., 1986).

Therefore, we interpret periods of dominance by *Aulacoseira* as reflecting high Si flux and enhanced mixing of the water column. Dominance by *Stephanodiscus* implies Si limitation, associated with either shallower mixing or a reduced hypolimnetic pool of Si (Stone et al., 2011). Enhanced Si flux from the catchment via streamflow would be expected under a more humid climate, whereas increased aridity would be expected to reduce the flux of Si from the landscape (Stager et al., 2003). Where diatom concentrations appear to be controlled primarily by production rather than dissolution or dilution, it is useful to examine concentrations of specific taxa, i.e., their absolute abundance, in addition to their relative abundance (Fig. 5) as variation in absolute abundance may be indicative of changes in the sizes of the nutrient pools.

Although *Aulacoseira* and *Stephanodiscus* species typically co-occurred, we observed significant variability in relative abundance over time. As each sample integrates multiple decades of sediment accumulation, the resulting assemblages reflect both seasonal variation in diatom community composition (succession) as well as interannual variability. Thus, our paleolimnological inferences from each sample refer to average conditions over 10s to 100s of years, and over thousands of years for each interval.

Aulacoseira was dominant in all intervals, although less frequently in Diatom Interval 6, suggesting complete mixing of the lakes during the diatom-producing freshwater phases was common. At 3.043 Ma (base of Interval 1), both the high relative abundance of *Aulacoseira* and its high concentration suggest that the lake was frequently well mixed. *Stephanodiscus* concentrations were also quite high (4.01×10^8 valves g^{-1}), implying the lake was not P-limited. By 3.037 Ma, the diminishing abundance of *Stephanodiscus* during a time when diatom production was relatively stable suggests a shift in resource ratios to greater Si:P, which could have resulted from extended strong mixing. Diatom Intervals 2 (2.991–2.986 Ma) and 3 (2.808 Ma) were overwhelmingly dominated by *Aulacoseira*, although strong dissolution may have biased the records of these freshwater phases. Nevertheless, the presence of *Aulacoseira* is evidence of deep mixing.

Interval 5 (2.658–2.655 Ma), the first of a sequence of four diatomites found in the upper 43 m of the core, was dominated by *Aulacoseira*, indicating strong mixing and high Si:P. The highest diatom concentrations in the interval correspond to increased relative abundance of *Stephanodiscus*. This suggests ambient nutrient levels were higher in addition to shifts in the ratio of Si:P associated with changes in mixing patterns. Concentrations of both *Aulacoseira* and *Stephanodiscus* increased in these samples, but it was an increase in *Aulacoseira* that drove peak production as inferred from valve concentration.

Significant shifts between dominance of *Aulacoseira* and *Stephanodiscus* occurred in Diatom Interval 6. Since detrital components are low and valve preservation is excellent in most of Interval 6, variation in valve concentration likely reflects variable production associated with ambient nutrient levels. Notably, the high diatom concentrations observed in this unit are associated with both higher absolute abundances of *Aulacoseira* and *Stephanodiscus* but are mainly driven by increases in *Stephanodiscus*, which suggests that Si supply remained high but that the supply of P relative to Si increased. This suggests something more than just shifting patterns in depth/strength of mixing. Possible causes include increased flux of P from the landscape or increased rate of internal P recycling. A decrease in mean lake depth could increase P flux from the sediments via increased disturbance of sediments and/or expansion of aquatic macrophytes (Reynolds and Davies, 2001).

The high relative abundance of *Stephanodiscus* observed in Diatom Interval 6 (as well as Diatom Interval 8) is comparable to the recent and Holocene assemblages of Lake Albert (Uganda/Democratic Republic of the Congo) (Kilham et al., 1986). However, the mechanism leading to low Si:P ratios in Lake Albert (Kilham et al., 1986) is different than the mechanism inferred for the Baringo paleolakes. The major inflows to Lake Albert, the Victoria Nile and Semliki rivers are sourced from Lake Victoria and Lake Edward, respectively. Both lakes function as sinks for Si, via sedimentation of diatoms, leading to reduced Si supply to Lake Albert (Kilham et al., 1986).

An increase in diatom concentration in Interval 7 at 2.609 Ma is associated primarily with an increase in *Aulacoseira* (Fig. 5), suggesting high Si:P ratios combined with high ambient nutrient levels, and a persistently well-mixed lake. Subsequently, diatom concentrations decreased and *Stephanodiscus* became a larger component of the assemblage, despite a decline in its absolute abundance. This suggests lower ambient nutrient levels in association with less frequent mixing of the whole water column resulting in falling Si:P ratios.

Early in Diatom Interval 8, at 2.588 Ma, the absolute abundance of both *Stephanodiscus* and *Aulacoseira* in the sediments increased, likely due to better preservation as lake levels rose and enhanced diatom production in response to higher ambient nutrient levels. High relative abundance of *Stephanodiscus* suggests lower Si:P ratios and shallower/weaker mixing on average. Subsequent reduction in valve concentration suggests lower diatom production, possibly due to shortened mixing seasons or a reduction in the hypolimnetic pool of nutrients. It is possible this reflects a shift to more stratified conditions on average. Although diatoms indicative of stratification are not observed, other algal groups may have replaced diatoms (see Ndebele-Murisa et al., 2010; Talling, 1966). When diatom concentrations increased at 2.586 Ma (9.71 mbs), both *Aulacoseira* and *Stephanodiscus* abundance increased, but *Stephanodiscus* dominated the assemblage, indicating more frequent mixing to supply nutrients to support increased diatom production but with a shift toward low Si:P on average.

The planktonic diatom assemblages of many East African lakes commonly include *Nitzschia* species. Planktonic or tychoplanktonic species of *Nitzschia* are observed in the sediments of Lake Victoria (Stager, 1984), Lake Albert (Kilham et al., 1986), Lake Naivasha (Bergner and Trauth, 2004) and Lake Baringo (present-day) (Owen, 1981). In BTB13-1A, periphytic *Nitzschia* were rarely observed and an unidentified *Nitzschia* that is likely planktonic based on its morphology was observed only in Interval 6 and in relative abundances of less than 2.5%. Planktonic *Nitzschia* taxa are associated with stratification in Lake Victoria (Hecky, 1993; Stager et al., 2003), often co-occurring with cyanophytes (Hecky and Kilham, 1973; Kilham et al., 1986). The relative unimportance of *Nitzschia* in the BTB13A-1A core as well as lack of other stratification indicators (e.g., cyclotelloid diatoms) suggests the diatomaceous lacustrine intervals were not typically stratified.

Cyclotella meneghiniana was observed infrequently, but is a significant component of the base of two diatomite units (Intervals 6 and 8; Fig. 4). Cyclotelloid diatoms are commonly found in low to very low nutrient environments, although *C. meneghiniana* is often observed in shallow, nutrient-rich waters (Lowe and Kheiri, 2015). *Cyclotella meneghiniana* has been observed as a dominant taxon in alkaline lakes in East Africa (Hecky and Kilham, 1973), where it was found over a relatively wide range of alkalinities up to ~40 meq/L and may be considered euryhaline. In a study of modern wetlands in the Bogoria-Baringo region, Owen et al. (2004) observed *C. meneghiniana* in the littoral zone of hypersaline Lake Bogoria. In large lakes, *C. meneghiniana* and related taxa are found where salinity fluctuates rapidly between fresh and brackish conditions (Stoermer and Yang, 1969; Tuchman et al., 1984). The presence of a species tolerant of a wide range of salinities at the base of freshwater diatomites is evidence for a transition from an alkaline/saline to freshwater lake. Diatom Intervals 6 and 8 are both associated with relatively thick packages of sediment (1.8 and 1.6 m, respectively) between the sequence boundary and transgressive surface, which we interpret as lowstand lake deposits before major flooding of the basin (Fig. 2). Variable salinity might be expected under a humid climate following arid periods as lake levels rise (Stone et al., 2011). During this transitional period, chemical differences between hypolimnetic and surface waters would have enhanced stratification, reduced mixing, and limited nutrient flux to the epilimnion.

In addition to *Aulacoseira* (67%) and *C. meneghiniana* (13%), the basal assemblage of Interval 8 (2.589 Ma) includes 14% *Encyonema* cf. *muelleri* and 5% other periphytic taxa. *Encyonema muelleri* is usually periphytic, although it can be found in the plankton of shallow lakes (Gasse, 1986). In East Africa, Gasse (1986) observed *E. muelleri* to have a wide tolerance for pH and alkalinity but a preference for moderately concentrated alkaline water. This assemblage reflects rising lake levels and freshening but the high fraction of periphytic taxa suggests a relatively shallow environment and possibly more gradually rising lake levels compared to other transgressive events.

Although *C. meneghinana* was not observed in Interval 7, the basal assemblage of this interval (2.610 Ma) features an elevated periphytic component (5%), which might reflect decreased production of planktonic taxa and/or greater proximity to littoral habitats of a shallower lake. This interpretation is consistent with the stratigraphic lake packaging (Scott et al., this issue), as this sample reflects the composition related to initial lake flooding.

Diatom Intervals 2 (2.991–2.986 Ma) and 3 (2.808 Ma) are characterized by poor preservation (high % ringleistes) and, in the case of Interval 2, lower concentrations than the other, unaltered intervals. Although characterized by freshwater planktonic assemblages, increased dissolution suggests higher alkalinity and lower lake levels compared to other intervals. More than 4.5 m of profundal and sublittoral sediment below Interval 2 was likely deposited in highly alkaline and/or saline lake water (Scott et al., this issue). Low but elevated percentages of periphytic taxa in Interval 2 may reflect a position nearer to shore and/or greater fluvial influence. Although sedimentation rates were low (Deino et al., this issue), and influx of clastic material had not increased appreciably, a large spike in riverweed (*Tristicha trifaria*) phytoliths in this interval suggests proximity to an inflowing river (Yost et al., this issue).

5.3. Lake mixing and climate

In the diatom-bearing lacustrine units of the BTB13-1A core, we have evidence for the development of relatively deep, freshwater lake phases that persisted for millennia at a time. The assemblages of the individual diatomite and diatomaceous mud intervals show remarkable similarity, being dominated consistently by species of *Aulacoseira* and/or *Stephanodiscus*. However, the different resource requirements of these two groups and the strong variation in relative abundance between them over time, implies significant changes in nutrient availability driven by lake processes (mixing, internal P recycling) and/or catchment processes (weathering and transport). These processes are in turn influenced by climate (Fritz, 1996). Although the multiple possible pathways limit our ability to identify the particular climate changes that drove the inferred paleolimnological changes, we can postulate several possible scenarios that may be further supported or refuted by other lines of evidence.

In shallow equatorial lakes where thermal stratification is only weakly developed, the thickness of the mixed layer will depend primarily on windiness (Lewis, 1987). Chemical stratification, with more ionically concentrated bottom waters, may also sometimes develop and inhibit deep mixing in lakes. When we infer from the diatoms that mixing was strong and the mixed layer was deep (*Aulacoseira* > > *Stephanodiscus*; high Si:P), this could indicate strong winds, which would also limit the development of stratification. This interpretation is, however, complicated by the fact that changes in local and/or regional hydroclimate would also be expected to alter nutrient

availability in the lake. For example, increased precipitation should enhance the weathering and transport of Si to the lake, favoring *Aulacoseira*. With respect to nutrient recycling, a decrease in the mean depth of the lake would be expected to increase P, which is recycled at a faster rate from wind-mixed littoral sediments (Reynolds and Davies, 2001). Depending on the morphology of the basin, such a change in mean lake depth could be associated with expansion or contraction of a lake. For these reasons, it is important to consider not only variability in relative abundance of taxa but also diatom concentration (or other measures of productivity) as it may provide information about changing nutrient loads over time.

In an analysis of the oxygen isotopes of biogenic silica from the outcrop diatomite corresponding to Interval 7, Wilson et al. (2014) concluded that $\delta^{18}O$ of silica recorded variability in the balance between evaporation and precipitation with millennial-scale cyclicity of 1400–1700 years. The isotope record is weakly, but significantly, correlated to the relative abundance of *Stephanodiscus*, with drier conditions corresponding to higher % *Stephanodiscus* (Wilson et al., 2014). This suggests a correspondence between wetter and windier conditions, although enhanced precipitation may have also increased Si flux from the catchment (Stager et al., 2003), which would have favored *Aulacoseira* by increasing the Si:P ratio.

5.4. Paleolake development

The diatom record of the BTB13-1A core suggests a major shift in depositional environments within the Baringo Basin at ~3.04 Ma (132 mbs). In sediments older than ~3.04 Ma, we observed diatoms only in very low concentrations, most likely a consequence of dilution by clastic sediment although dissolution in some intervals is a possibility. Similarly, phytolith fluxes (phytoliths cm^{-2} yr^{-1}) are very low below 132 mbs even when preservation of the microfossils is good (Yost et al., this issue). Fish fossils are also rarely observed in the lower part of the BTB13-A core, and only become abundant above 122 m (Billingsley et al., this issue). Most of the diatoms observed below 132 mbs belong to the freshwater genus *Aulacoseira*, although freshwater periphytic (attached) taxa are also occasionally present. Sedimentary facies (Scott et al., this issue) are interpreted to represent relatively thin packages of alluvial, fluvial, deltaic, wetland, and lacustrine sediments below 132 mbs. Even when the sedimentology indicates profundal to sublittoral lacustrine environments, diatoms are not abundant. Phytolith assemblages during this period feature xeric grasses and evidence of transient riparian or gallery forests (Yost et al., this issue). We interpret the interval before ~3.04 Ma as representing mainly alluvial plain to lake-marginal depositional environments with only brief intervals representing deeper lacustrine settings.

In sediments dating from ~3.04–2.56 Ma, diatom-rich intervals alternate with intervals where diatoms are absent or very poorly preserved. With few exceptions, the diatom-rich units feature distinctly freshwater, planktonic (free-floating) assemblages composed of species from the genera *Aulacoseira* and *Stephanodiscus*. Enhanced diatom dissolution, evidenced by microscopic observation of valve corrosion (e.g., Fig. 3Q), characterizes the upper parts of Diatom Intervals 1 and 5–8. In most cases, dissolution is reflected by increased % ringleistes and low concentrations (Fig. 6). However, it is low concentration that is indicative of increased dissolution at the top of Diatom Interval 6, which is dominated by *Stephanodiscus*. Diatom Intervals 2 and 3 contain evidence of significant dissolution throughout, whereas Diatom Interval 4 shows evidence of post-depositional alteration.

High alkalinity enhances the dissolution of biogenic silica. Thus, dissolution of diatoms in the upper parts of intervals indicates repeated shifts toward greater alkalinity and lower lake levels, which were likely driven by enhanced evaporation and/or decreased freshwater input to the lake associated with increased aridity. We did not observe corresponding shifts in the diatom assemblages that would indicate that the lake packages became shallower and/or more saline in the upper parts of these intervals, which suggests that the lakes remained relatively deep during initial increases in alkalinity.

Phytoliths show similar patterns of dissolution across the diatom intervals (Yost et al., this issue). Increased fluxes of sponge spicules and spheraster are also associated with enhanced diatom dissolution (Fig. 6), suggesting a preference for alkaline water by the sponges that produced them (Yost et al., this issue). In intervals where biogenic silica microfossils are absent or poorly preserved, authigenic zeolites are often present (Minkara et al., this issue). In Fig. 6, we plot the occurrence of the Na-bearing zeolite analcime, which is indicative of extremely saline alkaline ground or lake water (Hay, 1966; Renaut, 1993; Surdam and Sheppard, 1978). Analcime commonly forms in alkaline brines with high Na^+ activity and relatively low Si activity, most commonly in concentrated lake waters or proximal to hot springs hosting saline alkaline groundwater (Chipera and Apps, 2001; Hay and Sheppard, 2001; Langella et al., 2001). Additional zeolites (e.g., clinoptilolite/heulandite) representing less saline lake waters were also observed where diatoms are rare (see Minkara et al., this issue). Gradual increases in grain-size from silt to fine-grained sandstone above diatomaceous sediments in the upper set of lake packages (Diatom Intervals 4–8) reflects progradation of clastics into the increasingly shallow lakes before analcime cementation (Scott et al., this issue).

Together, the diatoms and other paleoenvironmental indicators suggest a major shift at ~3.04 Ma from a basin characterized by alluvial and shallow lake environments to one that, at times, featured relatively deep, freshwater lakes (Fig. 7). Changes in lake water alkalinity as inferred from the variable preservation of biogenic silica microfossils and presence of multiple zeolites indicative of mildly to strongly saline conditions together suggest that the lakes switched between hydrologically open and closed as lake levels rose and fell. The inferred lake level variability was most likely caused by variability in hydroclimate. The influence of climate on lake development within the Baringo Basin during the late Pliocene is supported by the precessional periodicity (~23 kyr) of the upper diatom-bearing units (Intervals 4–8), which was first documented by Deino et al. (2006). The deep, freshwater phases correspond most closely to June/July 30°N insolation maxima indicating moisture availability in the region was controlled by the African monsoon (Kingston et al., 2007). Further discussion of orbital forcing of sedimentation and terrestrial vegetation in the Baringo Basin can be found in Deino et al., this issue, Scott et al. (this issue), and Yost et al. (this issue).

The diatom record after ~3.04 Ma can be divided into an early period (~3.04–2.99 Ma) that featured two deep freshwater lake phases (Intervals 1 and 2). This was followed by a long middle period (~2.99–2.68 Ma) when diatoms were only sparsely recorded except for a brief interval at ~2.81 Ma (Interval 3), suggesting generally lower lake levels and a more arid climate and/or the development of a closed lake basin. This is supported by the phytolith record, which also features poor preservation during this interval, but indicates the presence of wetland plants, reflecting low water levels, and water-stressed grasses (Yost et al., this issue). A late period (~2.68–2.58 Ma) was characterized by at least four deep freshwater lake phases (Intervals 5–8) that alternated with marginal lacustrine and subaerially exposed environments (Scott et al., this issue). Interval 4, featuring low absolute abundances of altered *Aulacoseira,* probably represents a fifth freshwater lake phase during this period. Fluctuating lake levels may reflect strong hydroclimate variability or a climatically sensitive lake system where relatively moderate changes in precipitation produced rapid, amplified lake responses (Trauth et al., 2010).

6. Conclusions

The diatom record of the BTB13-1A core shows evidence of multiple lake highstands during the late Pliocene. During highstands, the lakes were dominated by freshwater planktonic species of *Aulacoseira* and *Stephanodiscus*. Species composition and diatom concentrations indicate

a moderate to high supply of silica and phosphorus. We infer that assemblages dominated by *Aulacoseira* represent a well-mixed lake and windier conditions. When *Stephanodiscus* was dominant, we infer incomplete mixing and weaker or shorter duration winds. *Aulacoseira* tended to dominate or co-dominate assemblages, except for the longest interval (Interval 6; 2.618–2.635 Ma) where *Stephanodiscus* was initially co-dominant and then came to dominate the assemblage. High diatom concentration and thus enhanced diatom production in Diatom Interval 6 is associated with high relative abundance of *Stephanodiscus*, suggesting the interval featured periods of increased flux of phosphorus.

Freshwater diatomaceous sediments alternate with sediments that include authigenic zeolites (e.g., analcime) indicative of alkaline and saline lake or groundwater, which implies that the Baringo Basin experienced significant environmental variability during this time. Dissolution of freshwater, planktonic diatom assemblages at the tops of diatomites suggests lake regressions were associated with relatively rapid transitions to higher alkalinity. Other than transitional assemblages suggestive of saline conditions during two lake transgressive events (Intervals 6 and 8), no littoral, saline, or alkaline diatom assemblages were preserved in the record.

Diatomaceous sediments indicative of deep, freshwater lakes were deposited only after ~3.04 Ma. Prior to ~3.04 Ma, concentrations of diatoms are very low, which is consistent with primarily fluvial and deltaic depositional environments. Five diatomites and one diatom-rich interval provide evidence for six main freshwater lake phases, ranging in length from ~3000 to 17,000 years. The first two freshwater phases occurred between 3.04 and 2.99 Ma. This was followed by a long period from 2.99 to 2.68 Ma with scant diatom evidence for freshwater lakes. A single sample at ~2.81 Ma may represent a brief freshwater phase. Between 2.68 to 2.58 Ma, four freshwater phases occurred, the longest lasting ~17,000 years. An interval at 2.68 Ma, which we interpret as a potentially diagenetically altered diatomite, would represent a fifth freshwater phase.

Acknowledgments

This research was conducted as part of the Hominin Sites and Paleolakes Drilling Program (HSPDP). Initial core processing and sampling was carried out at the National Lacustrine Core Facility (LacCore) which houses the cores. Funding for this work was provided by National Science Foundation (NSF; United States) grants EAR-1123942, BCS-1241859, EAR-1338553, and the International Continental Scientific Drilling Program (ICDP). M.S. acknowledges support from the Swiss National Science Foundation grant P300P2_158501 (SNF; Switzerland). We are grateful for discussions with HSPDP colleagues Anne Billingsley, Alan Deino, Daniel Deocampo, Rachel Lupien, and Karim Minkara. We thank Robert Edgar for providing microscope slides from the Barsemoi diatomites for comparison. We thank Sabrina Brown, Kendra Reininga, Ellie Gaskill, Emily Brana, Helena Bierly, and Erika Smith for assistance in subsampling, processing samples and preparing slides. We also thank two anonymous reviewers for valuable comments that improved the manuscript. This is publication #19 of the Hominin Sites and Paleolakes Drilling Project.

Appendix A. Supplementary data

Supplementary data to this article can be found online at https://doi.org/10.1016/j.palaeo.2019.109382.

References

Battarbee, R.W., Jones, V.J., Flower, R.J., Cameron, N.G., Bennion, H., Carvalho, L., Juggins, S., 2001. Diatoms. In: Smol, J.P., Birks, H.J.B., Last, W.M. (Eds.), Tracking Environmental Change Using Lake Sediments. Volume 3: Terrestrial, Algal, and Siliceous Indicators. Kluwer Academic Publishers, Dordrecht, The Netherlands, pp. 155–202.

Bergner, A.G.N., Trauth, M.H., 2004. Comparison of the hydrological and hydrochemical evolution of Lake Naivasha (Kenya) during three highstands between 175 and 60 kyr BP. Palaeogeogr. Palaeoclimatol. Palaeoecol. 215, 17–36. https://doi.org/10.1016/j.palaeo.2004.07.033.

Billingsley, A.L., Reinthal, P.N., Dettman, D.L., Deino, A.L., Ortiz, K., Mohler, B., Cohen, A.S., this issue. δ13C records from fish fossils as paleo-indicators of ecosystem responses to lake levels in the Plio-Pleistocene lakes of Tugen Hills, Kenya. Palaeogeogr. Palaeoclimatol. Palaeoecol.

Brown, E.T., Johnson, T.C., Scholz, C.A., Cohen, A.S., King, J.W., 2007. Abrupt change in tropical African climate linked to the bipolar seesaw over the past 55,000 years. Geophys. Res. Lett. 34, L20702. https://doi.org/10.1029/2007GL031240.

Burnett, A.P., Soreghan, M.J., Scholz, C.A., Brown, E.T., 2011. Tropical East African climate change and its relation to global climate: a record from Lake Tanganyika, Tropical East Africa, over the past 90+kyr. Palaeogeogr. Palaeoclimatol. Palaeoecol. 303, 155–167. https://doi.org/10.1016/j.palaeo.2010.02.011.

Campisano, C.J., Cohen, A.S., Arrowsmith, J.R., Asrat, A., Behresmeyer, A.K., Brown, E.T., Deino, A.L., Deocampo, D., Feibel, C.S., Kingston, J., Lamb, H.F., Lowenstein, T.K., Noren, A.J., Olago, D.O., Owen, R.B., Pelletier, J.D., Potts, R., Reed, K.E., Renaut, R.W., Russell, J.M., Russell, J.L., Shäbitz, F., Stone, J.R., Trauth, M.H., Wynn, J.G., 2017. The hominin sites and paleolakes drilling project: high-resolution paleoclimate records from the East African Rift System and their implications for understanding the environmental context of hominin evolution. PaleoAnthropology 2017, 1–43. https://doi.org/10.4207/PA.2017.ART104.

Chapman, G.R., 1971. The Geological Evolution of the Northern Kamasia Hills, Baringo District, Kenya (Doctoral Dissertaion). University of London.

Chapman, G.R., Brook, M., 1978. Chronostratigraphy of the Baringo Basin, Kenya. Geol. Soc. London, Spec. Publ. 6, 207–223. https://doi.org/10.1144/GSL.SP.1978.006.01.16.

Chapman, G.R., Lippard, S.J., Martyn, J.E., 1978. The stratigraphy and structure of the Kamasia Range, Kenya Rift Valley. J. Geol. Soc. London. 135, 265–281. https://doi.org/10.1144/gsjgs.135.3.0265.

Chipera, S.J., Apps, J.A., 2001. Geochemical stability of natural zeolites. Rev. Mineral. Geochem. 45, 117–161. https://doi.org/10.2138/rmg.2001.45.3.

Cohen, A.S., 2003. Paleolimnology: the History and Evolution of Lake Systems. Oxford University Press.

Cohen, A.S., Campisano, C., Arrowsmith, R., Asrat, A., Behrensmeyer, A.K., Deino, A., Feibel, C., Hill, A., Johnson, R., Kingston, J., Lamb, H., Lowenstein, T., Noren, A., Olago, D., Owen, R.B., Potts, R., Reed, K., Renaut, R., Schäbitz, F., Tiercelin, J.J., Trauth, M.H., Wynn, J., Ivory, S., Brady, K., O'Grady, R., Rodysill, J., Githiri, J., Russell, J., Foerster, V., Dommain, R., Rucina, S., Deocampo, D., Russell, J., Billingsley, A., Beck, C., Dorenbeck, G., Dullo, L., Feary, D., Garello, D., Gromig, R., Johnson, T., Junginger, A., Karanja, M., Kimburi, E., Mbuthia, A., McCartney, T., McNulty, E., Muiruri, V., Nambiro, E., Negash, E.W., Njagi, D., Wilson, J.N., Rabideaux, N., Raub, T., Sier, M.J., Smith, P., Urban, J., Warren, M., Yadeta, M., Yost, C., Zinaye, B., 2016. The Hominin Sites and Paleolakes Drilling Project: inferring the environmental context of human evolution from eastern African rift lake deposits. Sci. Drill. 21, 1–16. https://doi.org/10.5194/sd-21-1-2016.

De Cort, G., Verschuren, D., Ryken, E., Wolff, C., Renaut, R.W., Creutz, M., Van der Meeren, T., Haug, G., Olago, D.O., Mees, F., 2018. Multi-basin depositional framework for moisture-balance reconstruction during the last 1300 years at Lake Bogoria, central Kenya Rift Valley. Sedimentology 65, 1667–1696. https://doi.org/10.1111/sed.12442.

Deino, A.L., Hill, A., 2002. 40Ar/39Ar dating of Chemeron Formation strata encompassing the site of hominid KNM-BC 1, Tugen Hills, Kenya. J. Hum. Evol. 42, 141–151. https://doi.org/10.1006/JHEV.2001.0522.

Deino, A.L., Tauxe, L., Monaghan, M., Hill, A., 2002. 40Ar/39Ar geochronology and paleomagnetic stratigraphy of the Lukeino and lower Chemeron Formations at Tabarin and Kapcheberek, Tugen Hills, Kenya. J. Hum. Evol. 42, 117–140. https://doi.org/10.1006/JHEV.2001.0521.

Deino, A.L., Kingston, J.D., Glen, J.M., Edgar, R.K., Hill, A., 2006. Precessional forcing of lacustrine sedimentation in the late Cenozoic Chemeron Basin , Central Kenya Rift , and calibration of the Gauss/Matuyama boundary. Earth Planet. Sci. Lett. 247, 41–60. https://doi.org/10.1016/j.epsl.2006.04.009.

Deino, A.L., Sier, M.J., Garello, D.I., Keller, B., Kingston, J.D., Scott, J.J., Dupont-Nivet, G., Cohen, A.S., this issue. Chronostratigraphy of the Baringo-Tugen-Barsemoi (HSPDP-BTB13-1A) Core – 40Ar/39Ar dating, magnetostratigraphy, tephrostratigraphy, and Bayesian age modeling. Palaeogeogr. Palaeoclimatol. Palaeoecol.

Evans, J.H., 1997. Spatial and seasonal distribution of phytoplankton in an African rift valley lake (L. Albert, Uganda, zaire). Hydrobiologia 354, 1–16. https://doi.org/10.1023/A:1003026415788.

Fritz, S.C., 1996. Paleolimnological records of climatic change in North America. Limnol. Oceanogr. 41, 882–889. https://doi.org/10.4319/lo.1996.41.5.0882.

Gasse, F., 1980. Les diatomées lacustres Plio-Pléistocenes du Gadeb (Éthiopie) : systématique, paléoécologie, biostratigraphie. Revue Algologique Mémoire 3 (Paris).

Gasse, F., 1986. East African diatoms: taxonomy, ecological distribution. Bibl. Diatomol. 11 (J. Cramer, Stuttgart).

Gasse, F., Talling, J.F., Kilham, P., 1983. Diatom assemblages in East Africa : classification, distribution and ecology. Rev. d'Hydrobiologie Trop. 16, 3–34.

Gasse, F., Barker, P.A., Johnson, T.C., 2002. A 24,000 yr diatom record from the northern basin of Lake Malawi. In: Odada, E.O., Olago, D.O. (Eds.), East African Great Lakes: Limnology, Paleaeolimnology, and Biodiversity. Kluwer Academic Publishers, pp. 394–413.

Haberyan, K.A., 1987. Fossil diatoms and the paleolimnology of Lake Rukwa, Tanzania. Freshw. Biol. 17, 429–436. https://doi.org/10.1111/j.1365-2427.1987.tb01064.x.

Haberyan, K.A., Hecky, R.E., 1987. The late Pleistocene and Holocene stratigraphy and paleolimnology of lakes Kivu and Tanganyika. Palaeogeogr. Palaeoclimatol. Palaeoecol. 61, 169–197. https://doi.org/10.1016/0031-0182(87)90048-4.

Haberyan, K.A., Mhone, O.K., 1991. Algal communities near Cape Maclear, southern Lake Malawi, Africa. Hydrobiologia 215, 175–188. https://doi.org/10.1007/BF00764853.

Harwood, D.M., 2010. Diatomite. In: Stoermer, E.F., Smol, J.P. (Eds.), The Diatoms: Applications for the Environmental and Earth Sciences. Cambridge University Press, pp. 570–573.

Hautot, S., Tarits, P., Whaler, K., Le Gall, B., Tiercelin, J.-J., Le Turdu, C., 2000. Deep structure of the Baringo Rift Basin (central Kenya) from three-dimensional magnetotelluric imaging: implications for rift evolution. J. Geophys. Res. Solid Earth 105, 23493–23518. https://doi.org/10.1029/2000JB900213.

Hay, R.L., 1966. Zeolites and Zeolitic Reactions in Sedimentary Rocks (GSA Special Paper N. 85). Geological Society of America, New York.

Hay, R.L., Sheppard, R.A., 2001. Occurrence of zeolites in sedimentary rocks: an overview. Rev. Mineral. Geochem. 45, 217–234. https://doi.org/10.2138/rmg.2001.45.6.

Hecky, R.E., 1993. The eutrophication of Lake Victoria. Int. Vereinigung für Theor. und Angew. Limnol. Verhandlungen 25, 39–48. https://doi.org/10.1080/03680770.1992.11900057.

Hecky, R.E., Kilham, P., 1973. Diatoms in alkaline, saline lakes: ecology and geochemical implications. Limnol. Oceanogr. 18, 53–71. https://doi.org/10.4319/lo.1973.18.1.0053.

Hecky, R.E., Kling, H.J., 1987. Phytoplankton ecology of the great lakes in the rift valleys of central Africa. Arch. für Hydrobiol. Beihefte Ergebnisse der Limnol. 25, 197–228.

Hill, A., 1985. Early hominid from Baringo, Kenya. Nature 315, 222–224. https://doi.org/10.1038/315222a0.

Hill, A., 1995. Faunal and environmental change in the Neogene of East Africa: evidence from the Tugen Hills sequence, Baringo district, Kenya. In: Vrba, E.S., Denton, G.H., Partridge, T.C., Burckle, L.H. (Eds.), Paleoclimate and Evolution with Emphasis on Human Origins. Yale University Press, pp. 178–193.

Hill, A., 1999. The Baringo Basin, Kenya: from bill bishop to BPRP. In: Andrews, P., Banham, P. (Eds.), Late Cenozoic Environments and Hominid Evolution: A Tribute to Bill Bishop. The Geological Society, London, pp. 85–97.

Hill, A., Curtis, G., Drake, R., 1986. Sedimentary stratigraphy of the Tugen Hills, Baringo, Kenya. Geol. Soc. London, Spec. Publ. 25, 285–295. https://doi.org/10.1144/GSL.SP.1986.025.01.23.

Houk, V., 2003. Atlas of Freshwater Centric Diatoms with a Brief Key and Descriptions. Part I. Melosiraceae, Orthoseiraceae, Paraliaceae and Aulacoseiraceae., Czech Phycology Supplement. Czech Phycological Society, Olomouc.

Hubble, D.S., Harper, D.M., 2002. Phytoplankton community structure and succession in the water column of Lake Naivasha, Kenya: a shallow tropical lake. Hydrobiologia 488, 89–98. https://doi.org/10.1007/978-94-017-2031-1_8.

Jewson, D.H., 1992. Size reduction, reproductive strategy and the life cycle of a centric diatom. Philos. Trans. Biol. Sci. 336, 191–213. https://doi.org/10.1098/rstb.1992.0056.

Johnson, T.C., Brown, E.T., Shi, J., 2011. Biogenic silica deposition in Lake Malawi, East Africa over the past 150,000 years. Palaeogeogr. Palaeoclimatol. Palaeoecol. 303, 103–109. https://doi.org/10.1016/j.palaeo.2010.01.024.

Junginger, A., Trauth, M.H., 2013. Hydrological constraints of paleo-Lake Suguta in the Northern Kenya Rift during the African Humid Period (15–5kaBP). Glob. Planet. Chang. 111, 174–188. https://doi.org/10.1016/j.gloplacha.2013.09.005.

Kilham, P., 1971. A hypothesis concerning silica and the freshwater planktonic diatoms. Limnol. Oceanogr. 16, 10–18. https://doi.org/10.4319/lo.1971.16.1.0010.

Kilham, S.S., 1984. Silicon and phosphorus growth kinetics and competitive interactions between *Stephanodiscus minutus* and *Synedra* sp. Int. Vereinigung für Theor. und Angew. Limnol. Verhandlungen 22, 435–439. https://doi.org/10.1080/03680770.1983.11897326.

Kilham, S.S., 1986. Dynamics of Lake Michigan natural phytoplankton communities in continuous cultures along a Si:P loading gradient. Can. J. Fish. Aquat. Sci. 43, 351–360. https://doi.org/10.1139/f86-045.

Kilham, P., 1990. Ecology of *Melosira* species in the great lakes of Africa. In: Tilzer, M.M., Serruya, C. (Eds.), Large Lakes: Ecological Structure and Function. Springer-Verlag, Berlin, pp. 414–427.

Kilham, S.S., Kilham, P., 1975. *Melosira granulata* (Ehr.) Ralfs: morphology and ecology of a cosmopolitan freshwater diatom. Int. Vereinigung für Theor. und Angew. Limnol. Verhandlungen 19, 2716–2721. https://doi.org/10.1080/03680770.1974.11896368.

Kilham, P., Kilham, S.S., Hecky, R.E., 1986. Hypothesized resource relationships among African planktonic diatoms. Limnol. Oceanogr. 31, 1169–1181. https://doi.org/10.4319/lo.1986.31.6.1169.

Kilham, S.S., Theriot, E.C., Fritz, S., 1996. Linking planktonic diatoms and climate change in the large lakes of the Yellowstone ecosystem using resource theory. Limnol. Oceanogr. 41, 1052–1062. https://doi.org/10.4319/lo.1996.41.5.1052.

Kingston, J.D., Deino, A.L., Edgar, R.K., Hill, A., 2007. Astronomically forced climate change in the Kenyan Rift Valley 2.7-2.55 Ma: implications for the evolution of early hominin ecosystems. J. Hum. Evol. 53, 487–503. https://doi.org/10.1016/j.jhevol.2006.12.007.

Kingston, J.D., Deino, A.L., Cohen, A.S., this issue. Overview of goals and outcomes of the baringo-tugen Hills- Barsemoi (BTB) drill core, central Kenya rift valley. Palaeogeogr. Palaeoclimatol. Palaeoecol.

Kingston, J.D., Jacobs, B.F., Hill, A., Deino, A.L., 2002. Stratigraphy, age and environments of the late Miocene Mpesida Beds, Tugen Hills, Kenya. J. Hum. Evol. 42, 95–116. https://doi.org/10.1006/jhev.2001.0503.

Krammer, K., Lange-Bertalot, H., 1986. Süsswasserflora von Mitteleuropa, Band 2/1: Bacillariophyceae. 1. Teil: Naviculaceae. Gustav Fisher Verlag, Jena.

Krammer, K., Lange-Bertalot, H., 1991. Süsswasserflora von Mitteleuropa, Band 2/3: Bacillariophyceae. 3. Teil: Centrales, Fragilariaceae, Eunotiaceae. Gustav Fisher Verlag, Jena.

Laird, K.R., Cumming, B.F., 2009. Diatom-inferred lake level from near-shore cores in a drainage lake from the Experimental Lakes Area, northwestern Ontario, Canada. J. Paleolimnol. 42, 65–80. https://doi.org/10.1007/s10933-008-9248-9.

Laird, K.R., Kingsbury, M.V., Cumming, B.F., 2010. Diatom habitats, species diversity and water-depth inference models across surface-sediment transects in Worth Lake, northwest Ontario, Canada. J. Paleolimnol. 44, 1009–1024. https://doi.org/10.1007/s10933-010-9470-0.

Langella, A., Cappelletti, P., de' Gennaro, R., 2001. Zeolites in closed hydrologic systems. Rev. Mineral. Geochem. 45, 235–260. https://doi.org/10.2138/rmg.2001.45.7.

Le Turdu, C., Coussement, C., Tiercelin, J.-J., Renaut, R.W., Rolet, J., Richert, J.-P., Xavier, J.-P., Coquelet, D., 1995. Rift basin structure and depositional patterns interpreted using a 3D remote sensing approach: the Baringo and Bogoria Basins, central Kenya Rift, East Africa. Bull. Centres Rech. Explor. Elf Aquitaine 19, 1–37.

Lewis, W.M., 1987. Tropical limnology. Annu. Rev. Ecol. Systemat. 18, 159–184. https://doi.org/10.1146/annurev.es.18.110187.001111.

Lowe, R.L., Kheiri, S., 2015. Cyclotella meneghiniana. [WWW Document]. Diatoms North Am. URL. https://diatoms.org/species/cyclotella_meneghiniana (accessed 3.8.18).

Martyn, J.E., 1969. The Geological History of the Country between Lake Baringo and the Kerio River, Baringo District, Kenya. Doctoral Dissertation. University of London.

McCall, G.J.H., Baker, B.H., Walsh, J., 1967. Late Tertiary and Quaternary sediments of the Kenya rift valley. In: Bishop, W.W., Clark, J.D. (Eds.), Background to Evolution in Africa. University of Chicago Press, Chicago, pp. 191–220.

McQuoid, M.R., Hobson, L.A., 1996. Diatom resting stages. J. Phycol. 32, 889–902. https://doi.org/10.1111/j.0022-3646.1996.00889.x.

Minkara, K.E., Deocampo, D.M., Rabideaux, N.M., Kingston, J.D., Deino, A.L., Cohen, A.S., Campisano, C.J., this issue. Zeolite Facies and Implication for Environmental Change from the Chemeron Formation of the Baringo Basin, Kenya Rift, 3.3-2.6 Ma. Palaeogeogr. Palaeoclimatol. Palaeoecol.

Moos, M.T., Laird, K.R., Cumming, B.F., 2005. Diatom assemblages and water depth in Lake 239 (Experimental Lakes Area, Ontario): implications for paleoclimatic studies. J. Paleolimnol. 34, 217–227. https://doi.org/10.1007/s10933-005-2382-8.

Ndebele-Murisa, M.R., Musil, C.F., Raitt, L., 2010. A review of phytoplankton dynamics in tropical African lakes. South Afr. J. Sci. 106, 13–18.

Oduor, S.O., Schagerl, M., Mathooko, J.M., 2003. On the limnology of Lake Baringo (Kenya): I.temporal physico-chemical dynamics. Hydrobiologia 506, 121–127. https://doi.org/10.1023/B:HYDR.0000008563.00000.18.

Okech, E.O., Kitaka, N., Omondi, S., Verschuren, D., 2019. Water level fluctuations in Lake Baringo, Kenya, during the 19th and 20th centuries: evidence from lake sediments. Afr. J. Aquat. Sci. 44, 25–33. https://doi.org/10.2989/16085914.2019.1583087.

Olaka, L.A., Odada, E.O., Trauth, M.H., Olago, D.O., 2010. The sensitivity of East African rift lakes to climate fluctuations. J. Paleolimnol. 44, 629–644. https://doi.org/10.1007/s10933-010-9442-4.

Owen, R.B., 1981. Quaternary Diatomaceous Sediments and the Geological Evolution of Lakes, Turkana, Baringo and Bogoria Kenya Rift Valley. Doctoral dissertation. University of London.

Owen, R.B., Crossley, R., 1992. Spatial and temporal distribution of diatoms in sediments of Lake Malawi, Central Africa, and ecological implications. J. Paleolimnol. 7, 55–71. https://doi.org/10.1007/BF00197031.

Owen, R.B., Renaut, R.W., 2000. Miocene and Pliocene diatomaceous lacustrine sediments of the tugen Hills, Baringo district, Central Kenya rift. In: Gierlowski-Kordesch, E.H., Kelts, K.R. (Eds.), Lake Basins through Space and Time. American Association of Petroleum Geologists, pp. 465–472. https://doi.org/10.1306/St46706C42.

Owen, R.B., Renaut, R.W., Hover, V.C., Ashley, G.M., Muasya, A.M., 2004. Swamps, springs and diatoms: wetlands of the semi-arid Bogoria-Baringo Rift, Kenya. Hydrobiologia 518, 59–78. https://doi.org/10.1023/B:HYDR.0000025057.62967.2c.

Pilskaln, C.H., Johnson, T.C., 1991. Seasonal signals in Lake Malawi sediments. Limnol. Oceanogr. 36, 544–557. https://doi.org/10.4319/lo.1991.36.3.0544.

Piperno, D.R., 2006. Phytoliths: A Comprehensive Guide for Archaeologists and Paleoecologists. AltaMira Press, Lanham, MD.

Renaut, R.W., 1993. Zeolitic diagenesis of late Quaternary fluviolacustrine sediments and associated calcrete formation in the Lake Bogoria Basin, Kenya Rift Valley. Sedimentology 40, 271–301. https://doi.org/10.1111/j.1365-3091.1993.tb01764.x.

Renaut, R.W., Ego, J.K., Tiercelin, J.-J., Le Turdu, C., Owen, R.B., 1999. Saline, alkaline palaeolakes of the Tugen hills-Kerio Valley region, Kenya Rift Valley. In: Andrews, P., Banham, P. (Eds.), Recognizing Responses to Environmental Change; Late Cenozoic Environments and Hominid Evolution a Tribute to the Late Bill Bishop. Geological Society, Bath, pp. 41–58.

Renaut, R.W., Tiercelin, J.-J., 1994. Lake Bogoria, Kenya Rift Valley - a sedimentological overview. In: Renaut, R.W., Last, W.M. (Eds.), Sedimentology and Geochemistry of Modern and Ancient Saline Lakes. SEPM Society for Sedimentary Geology, pp. 101–123. https://doi.org/10.2110/pec.94.50.0101.

Renaut, R.W., Tiercelin, J.-J., Owen, R.B., 2000. Lake Baringo, Kenya Rift Valley, and its Pleistocene precursors. In: Gierlowski-Kordesch, E.H., Kelts, K.R. (Eds.), Lake Basins through Space and Time. American Association of Petroleum Geologists, pp. 561–568.

Reynolds, C.S., Davies, P.S., 2001. Sources and bioavailability of phosphorus fractions in freshwaters: a British perspective. Biol. Rev. 76, 27–64. https://doi.org/10.1111/j.1469-185X.2000.tb00058.x.

Schagerl, M., Oduor, S.O., 2003. On the limnology of Lake Baringo (Kenya): II. Pelagic primary production and algal composition of Lake Baringo, Kenya. Hydrobiologia 506, 297–303. https://doi.org/10.1023/B:HYDR.0000008562.97458.d1.

Scholz, C.A., King, J.W., Ellis, G.S., Swart, P.K., Stager, J.C., Colman, S.M., 2003. Paleolimnology of Lake Tanganyika, East Africa, over the past 100 k yr. J. Paleolimnol. 30, 139–150. https://doi.org/10.1023/A:1025522116249.

Scott, J.J., Chupik, D.T., Deino, A.L., Stockhecke, M., Kingston, J.D., Westover, K.S., Lukens, W.E., Deocampo, D.M., Yost, C.L., Billingsley, A.L., Minkara, K.E., Ortiz, K., Cohen, A.S., this issue. Sequence stratigraphic framework for lacustrine transgression-regression cycles in the 3.3–2.6 Ma interval of the Chemeron Formation BTB13 core, Baringo Basin, Kenya. Palaeogeogr. Palaeoclimatol. Palaeoecol.

Sicko-Goad, L., Stoermer, E.F., Fahnenstiel, G.L., 1986. Rejuvenation of *Melosira granulata* (Bacillariophyceae) resting cells from the anoxic sediments of Douglas Lake, Michigan. I. Light Microscopy and 14C uptake. J. Phycol. 22, 22–28. https://doi.org/10.1111/j.1529-8817.1986.tb02510.x.

Smol, J.P., Stoermer, E.F., 2010. Applications and uses of diatoms: prologue. In: Smol, J.P., Stoermer, E.F. (Eds.), The Diatoms: Applications for the Environmental and Earth Sciences. Cambridge University Press, Cambridge; New York, pp. 3–7.

Spaulding, S.A., Bishop, I.W., Edlund, M.B., Lee, S., Potapova, M., 2018. Diatoms of North America. [WWW Document]. URL. https://diatoms.org/.

Stager, J.C., 1984. The diatom record of Lake Victoria (East Africa): the last 17,000 years. In: Mann, D.G. (Ed.), Proceedings of the Seventh International Diatom Symposium. Koeltz, Koenigstein, Philadelphia, pp. 455–476.

Stager, J.C., Johnson, T.C., 2000. A 12,400 14 C yr offshore diatom record from east central Lake Victoria, East Africa. J. Paleolimnol. 23, 373–383. https://doi.org/10.1023/A:1008133727763.

Stager, J.C., Cumming, B.F., Meeker, L.D., 2003. A 10,000-year high-resolution diatom record from Pilkington Bay, Lake Victoria, East Africa. Quat. Res. 59, 172–181. https://doi.org/10.1016/S0033-5894(03)00008-5.

Stockhecke, M., Brown, E.T., Scott, J.J., Kingston, J.D., Cohen, A.S., Yost, C.L., Westover, K.S., Stone, J.R., this issue. A continental high-resolution record from the Baringo Basin during major global climate reorganizations based on X-ray fluorescence. Palaeogeogr. Palaeoclimatol. Palaeoecol.

Stoermer, E.F., Yang, J.J., 1969. Plankton Diatom Assemblages in Lake Michigan. Great Lakes Research Division Special Report No. 47. (Ann Arbor).

Stone, J.R., Fritz, S.C., 2004. Three-dimensional modeling of lacustrine diatom habitat areas: improving paleolimnological interpretation of planktic:benthic ratios. Limnol. Oceanogr. 49, 1540–1548. https://doi.org/10.4319/lo.2004.49.5.1540.

Stone, J.R., Westover, K.S., Cohen, A.S., 2011. Late Pleistocene paleohydrography and diatom paleoecology of the central basin of Lake Malawi, Africa. Palaeogeogr. Palaeoclimatol. Palaeoecol. 303, 51–70. https://doi.org/10.1016/j.palaeo.2010.01.012.

Surdam, R.C., Sheppard, R.A., 1978. Zeolites in saline, alkaline-lake deposits. In: Sand, L.B., Mumpton, F.A. (Eds.), Natural Zeolites: Occurrence, Properties, Use. Pergamon, Oxford, pp. 145–174.

Talling, J.F., 1966. The annual cycle of stratification and phytoplankton growth in Lake Victoria (East Africa). Int. Rev. der Gesamten Hydrobiol. und Hydrogr. 51, 545–621. https://doi.org/10.1002/iroh.19660510402.

Talling, J.F., 1986. The seasonality of phytoplankton in African lakes. Hydrobiologia 138, 139–160. https://doi.org/10.1007/BF00027237.

Tiercelin, J.-J., Lezzar, K.E., 2002. A 300 million years history of rift lakes in Central and East Africa: an updated broad review. In: Odada, E.O., Olago, D.O. (Eds.), The East African Great Lakes: Limnology, Palaeolimnology and Biodiversity. Kluwer Academic Publishers, Dordrecht, Netherlands, pp. 3–60.

Tiercelin, J.-J., Vincens, A., Barton, C.E., Carbonel, P., Casanova, J., Delibrias, G., Gasse, F., Grosdidier, E., Herbin, J.-P., Huc, A.Y., Jardiné, S., Le Fournier, J., Mélières, F., Owen, R.B., Pagé, P., Palacios, C., Paquet, H., Péniguel, G., Peypouqu, J.-P., Raynaud, J.-F., Renaut, R.W., Renéville, P., Richert, J.-P., Riff, R., Robert, P., Seyve, C., Vandenbrouke, M., Vidal, G., 1987. Le demi-grabin de Baringo-Bogoria, Rift Gregory, Kenya: 30 000 years of hydrological and sedimentary history. Bull. Centres Rech. Explor. Elf Aquitaine 11, 249–540.

Tiercelin, J.-J., Nalpas, T., Thuo, P., Potdevin, J.-L., 2012. Hydrocarbon prospectivity in Mesozoic and early–middle Cenozoic rift basins of central and northern Kenya, eastern Africa. In: Gao, D. (Ed.), Tectonics and Sedimentation: Implications for Petroleum Systems: AAPG Memoir 100. AAPG, pp. 179–207.

Tilman, D.G., Kilham, S.S., Kilham, P., 1982. Phytoplankton community ecology: the role of limiting nutrients. Annu. Rev. Ecol. Systemat. 13, 349–372. https://doi.org/10.1146/annurev.es.13.110182.002025.

Trauth, M.H., Maslin, M.a., Deino, A.L., Junginger, A., Lesoloyia, M., Odada, E.O., Olago, D.O., Olaka, L.A., Strecker, M.R., Tiedemann, R., 2010. Human evolution in a variable environment: the amplifier lakes of Eastern Africa. Quat. Sci. Rev. 29, 2981–2988. https://doi.org/10.1016/j.quascirev.2010.07.007.

Tuchman, M.L., Theriot, E., Stoermer, E.F., 1984. Effects of low level salinity concentrations on the growth of *Cyclotella meneghiniana* Kütz. (Bacillariophyta). Arch. Protistenkd. 128, 319–326. https://doi.org/10.1016/S0003-9365(84)80003-2.

Vilaclara, G., Rico, R., Miranda, J., 1997. Effects of perturbations on diatom assemblages in Tlaxcala Paleolake, Mexico. Verhandlungen Int. Vereinigung Limnol. 26, 846–851. https://doi.org/10.1080/03680770.1995.11900837.

Westover, K.S., Stone, J.R., 2019. Diatom Assemblage and Concentration Data for HSPDP-BTB13-1a (Baringo Basin, Kenya). Mendeley Data. https://doi.org/10.17632/vv9jdmj5xv.1.

Wilson, K.E., Maslin, M.A., Leng, M.J., Kingston, J.D., Deino, A.L., Edgar, R.K., Mackay, A.W., 2014. East African lake evidence for Pliocene millennial-scale climate variability. Geology 42, 955–958. https://doi.org/10.1130/G35915.1.

Wolin, J.A., Stone, J.R., 2010. Diatoms as indicators of water-level change in freshwater lakes. In: Stoermer, E.F., Smol, J.P. (Eds.), The Diatoms: Applications for the Environmental and Earth Sciences. Cambridge University Press, pp. 174–185.

Yost, C.L., Ivory, S.J., Deino, A.L., Rabideaux, N.M., Kingston, J.D., Cohen, A.S., this issue. Phytoliths, pollen, and microcharcoal from the Baringo Basin, Kenya reveal savanna dynamics during the Plio-Pleistocene transition. Palaeogeogr. Palaeoclimatol. Palaeoecol.